The role of low-temperature (off-axis) alteration of the oceanic crust in the global Li-cycle: Insights from the Troodos ophiolite

L.A. Coogan, K.M. Gillis, M. Pope, J. Spence

2017

The final published version of this article can be found at:

https://doi.org/10.1016/j.gca.2017.01.002

Citation for this paper:

Coogan, L.A., Gillis, K.M., Pope, M. & Spence, J. (2017). The role of low-temperature (off-axis) alteration of the oceanic crust in the global Li-cycle: Insights from the Troodos ophiolite. *Geochimica et Cosmochimica Acta*, 203, 201-215. https://doi.org/10.1016/j.gca.2017.01.002

The role of low-temperature alteration of the oceanic crust in the global Li-cycle: insights from the Troodos ophiolite

Submitted to GCA 20th May 2016

Revised manuscript returned 14th Dec 2016

[1]L.A. Coogan, [1]K.M. Gillis, [1]M. Pope, [1]J. Spence,

[1]School of Earth and Ocean Sciences, University of Victoria, Victoria, BC, Canada, V8P 5C2; Tel: (1) 250 472 4018; Fax: (1) 250 721 6200; lacoogan@uvic.ca

ABSTRACT

Changes in the global Li-cycle, as recorded in the Li concentration and/or isotopic composition of seawater, have the potential to provide important insight into the controls on the long-term C-cycle. Understanding the magnitude and isotopic composition of the fluxes of Li into and out-of the ocean, and the controls on any variability in these, is necessary if we are to correctly interpret the paleo-record of the Li-cycle. Here the low-temperature hydrothermal sink is investigated using the volcanic section of the exceptionally preserved Troodos ophiolite. Using glass to define the protolith Li content, the uptake flux of Li is determined using bulk-rock analyses from four hydrologically distinct sections through the lava pile of the ophiolite. Differences in paleo-hydrological conditions in the crust appear to have played a significant role in controlling the uptake

23 flux of Li with an 'average' uptake flux of equivalent to 14-21x10^{9} mol yr^{-1} – this is
24 considerably larger than generally assumed. Bulk-rock samples that contain a large
25 seawater Li component have δ^{7}Li of ~10±2‰. Celadonite separates have a δ^{7}Li of
26 ~6±1‰, considerably lighter than bulk-rock samples with the same Li content. Because
27 celadonite is a significant repository for Li within the Troodos upper crust this means that
28 another phase(s) must have markedly heavier δ^{7}Li than the average bulk-rock; i.e.
29 changes in the average mineralogy of altered crust will lead to changes in the bulk
30 isotopic fractionation between the Li added to the upper oceanic crust and seawater (Δ_{SW-}
31 $_{lava}$). The shallowest samples in three of the four studied sections are isotopically lighter
32 than deeper samples (but do not contain significant celadonite), again indicating that
33 variations in alteration conditions and/or mineralogy can lead to variations in $\Delta_{SW-lava}$.
34 Comparison with other studies of altered upper oceanic crust suggests that changes in
35 alteration conditions (probably largely temperature) lead to significant changes in $\Delta_{SW-lava}$.
36 These changes likely reflect both a temperature dependence of the isotopic fractionation
37 factor and a change in the fractionation factor due to changing mineral assemblage and/or
38 mineral compositions and abundances. A significant portion of the increase in δ^{7}Li of
39 seawater over the past 50 Myr may be due to an increase in the bulk fractionation factor
40 between seawater and Li added to the upper oceanic crust due to cooling bottom water.
41

1. INTRODUCTION

The small inventory of C in the ocean-atmosphere system relative to the solid earth means that, on a million year timescale, the C-fluxes between these reservoirs must be closely balanced to avoid massive changes in atmospheric CO_2 and hence large fluctuations in climate. Walker et al. (1981) proposed that a feedback between the rate of continental chemical weathering and atmospheric CO_2, driven largely by changes in temperature and precipitation, could act as a planetary thermostat. Substantial effort has gone into testing this model using both modern and ancient systems. The climatic effect on modern chemical weathering rate, based on river chemistry, has been widely investigated but a simple relationship has proved difficult to find (e.g. Gaillardet et al., 1999; Kump et al., 2000; West et al., 2005; White and Buss, 2014; although see Li et al., 2016). The climatic effect on ancient chemical weathering rates has been widely investigated by searching for links between paleo-ocean chemistry and climate. Until recently probably the most discussed approach used the change in seawater $^{87}Sr/^{86}Sr$ as a potential tracer for the extent of continental chemical weathering (e.g. Lowenstein et al., 2014). However, the increase in seawater $^{87}Sr/^{86}Sr$ over the past 40 Myr coincides with planetary cooling and hence is the inverse of that expected if continental chemical weathering extent decreased with climate cooling. Instead, this increase in $^{87}Sr/^{86}Sr$ is widely thought to reflect increased weathering of the Himalaya, which could be interpreted as a topographic (or "weatherability") rather than climatic control on weathering rates (e.g. Raymo and Ruddiman, 1992). However, the partitioning of the river Sr flux between silicate and carbonate weathering is complex leading to uncertainty

in this interpretation (e.g. Edmond, 1992; Bickle et al., 2001). An alternative model is that the increase in seawater $^{87}Sr/^{86}Sr$ over the last 40 Myr is due to cooling of the deep ocean leading to lower temperatures (Gillis and Coogan, 2011), and hence slower reaction rates, in off-axis hydrothermal systems in the upper oceanic crust (Coogan and Dosso, 2015). A similar explanation has been proposed to explain the Mg-isotopic composition of Cenozoic seawater (Higgins and Schrag, 2015). If these interpretations are correct, and low-temperature seafloor hydrothermal circulation acts as a major, climate sensitive, CO_2 sink (Brady and Gislasson, 1997; Coogan and Gillis, 2013; Mills et al., 2014) then continental chemical weathering rate and climate may not be strongly coupled.

The recent publication of a record of the Li-isotopic composition of Cenozoic seawater (δ^7Li_{SW}) has provided a new way to investigate paleo-weathering rates (Misra and Froelich, 2012). Lithium potentially provides a particularly useful tracer to look for a link between the breakdown of silicate minerals and CO_2 drawdown because, unlike Sr, most Li is held in silicate rocks not carbonates or evaporates (e.g. Stoffyn-Egli and Mackenzie, 1984; Seyfried et al., 1984). The concentration of Li in seawater, $[Li]_{SW}$, is not well constrained but appears to have stayed within about ±40% of its modern value (~180 ppb) over the last 100 Myr based on the Li content of foraminifera (Delaney and Boyle, 1985; Hathorne and James, 2005; Misra and Froelich, 2012). The Li-isotopic composition of seawater (δ^7Li_{SW}) has apparently increased ~8-9‰ over the last 60 Myr to the modern value of ~31‰ (Misra and Froelich, 2012). This change in δ^7Li_{SW} could provide important constraints on the long term C-cycle. However, although there has been decades of research into the chemical cycling of Li in the ocean (e.g. Seyfried et

al.,1984; Stoffyn-Egli and Mackenzie,1984) there are still major uncertainties in the magnitude and isotopic composition of the fluxes into and out-of the ocean. The primary aim of this study is to better constrain the magnitude of, and controls on, the Li and Li-isotopic flux into oceanic crust altered in low-temperature off-axis hydrothermal systems.

The main inputs of Li to the ocean are river waters and high-temperature hydrothermal fluids, and the main sinks are low-temperature alteration of the oceanic crust and sediment diagenesis (Fig. 1). Estimates of both the size of the Li fluxes, and their isotopic compositions, vary substantially (Fig. 1) as do models for which of these is most likely to have changed over the last 60 Myr to drive the change in δ^7Li_{SW}. For example, Misra and Froelich (2012) suggest that increasing δ^7Li_{SW} over the Cenozoic was largely driven by a change from congruent weathering (producing a river flux with a similar isotopic composition to average continental crust) to incongruent weathering with a river flux ~20‰ heavier than average continental crust. Alternatively, Li and West (2014) suggest that changes in the amount of Li taken up by diagenetic reactions in oceanic sediments played a key role in controlling the change in δ^7Li_{SW} and Vigier and Godderis (2015) argue that changing river Li fluxes, not their isotopic composition, were the key driver of the change in δ^7Li_{SW}. These models, and others, generally assume a largely constant uptake flux of Li during low-temperature alteration of the upper oceanic crust with a constant bulk Li-isotopic fractionation between seawater and the Li taken up by the rock ($\Delta_{SW\text{-}lava}$). Here we explore this uptake flux to investigate what the primary controls on this are, and whether variations in both the Li uptake flux and $\Delta_{SW\text{-}lava}$ may have occurred, providing an additional forcing on δ^7Li_{SW}.

Off-axis hydrothermal systems, driven by the cooling of the oceanic lithosphere, carry fluid fluxes of a similar magnitude to the river flux and operate across much of the ocean basins (e.g. Fisher, 2005). Water-to-rock ratios in these systems are typically of the order of 1000-2000 (e.g. Coogan and Gillis, 2013). In off-axis hydrothermal systems fluid generally enters the crust where high permeability lavas are exposed at the seafloor and most fluid flow occurs within the lava section of the crust referred to as the crustal aquifer (e.g. Fisher and Wheat, 2012). Fluid recharge into the crustal aquifer through any significant thickness of sediment is negligible (a few percent of the flux) due to the much lower permeability of abyssal sediments than lavas (Spinelli et al., 2004; Anderson et al., 2014); i.e. the fluid recharging the crustal aquifer is largely unmodified seawater. The fluid in the crust is, on average, heated only ~10°C, meaning that the temperature of ocean bottom water plays a strong role in controlling the temperature of fluid-rock reaction within off-axis hydrothermal systems (Gillis and Coogan, 2011). However, where sediment is thick (e.g. 100's of m) it acts as a thermal blanket and higher temperatures can be achieved in the crust. The extent of chemical exchange between the crust and ocean in off-axis systems has been hypothesized to be dependent on bottom water temperature based on the C content of oceanic crust (Gillis and Coogan, 2011), the Mg-isotope record of seawater (Higgins and Schrag, 2015), and the Sr-isotopic composition of void filling carbonate within the upper oceanic crust (Coogan and Dosso, 2015). However, there are strong small-scale hydrological controls on crustal alteration due to variations in seafloor topography and sedimentation history (e.g. Gillis and Robinson, 1988; Fisher, 2005; Anderson et al., 2012; Gillis et al., 2015).

Our current constraints on the uptake of Li from the ocean in off-axis hydrothermal systems are limited and come from three disparate, and non-typical, hydrological settings. In a study widely used to define the bulk isotope fractionation factor during low-temperature alteration, Chan et al. (1992) measured the Li content and isotopic composition of samples dredged from the seafloor in the Atlantic along a time line from 0 to 46 Myr old crust. Because dredging only samples the seafloor these data reflect alteration at, or very near, the top of the oceanic crust in locations not buried by significant sediment and thus are far from typical of the upper oceanic crust. These samples show a strong linear correlation of 1/Li with δ^7Li with an altered end-member of ~14‰ (blue symbols in Fig. 1). This end-member does not change if only samples <10 Myr old are considered, leading to the conclusion that $\Delta_{SW\text{-}lava}$ under bottom-water conditions over the last 10 Myr is ~16 to 17‰ (Chan et al., 2002; Misra and Froelich, 2012). The second detailed study of Li in altered upper oceanic crust is of samples from ~6.6 Myr old crust, drilled at the adjacent ODP Sites 504 and 896 (Chan et al., 2002) in an area of rapid sedimentation (~40 m Myr^{-1}) and hence warm crustal temperature. These samples appear to define $\Delta_{SW\text{-}lava}$ ~8-10‰ (red symbols in Fig. 1), much smaller than from the dredge samples, perhaps because the crust was altered under warm conditions. The final robust dataset for upper oceanic crust altered in off-axis hydrothermal systems comes from IODP Site 1256 (Gao et al., 2012) where there appears to have been little Li added to the crust (and Li loss from some lavas) and there is no obvious single "altered end-member". This site was also rapidly sedimented and has a >75 m thick ponded lava capping the section that will have acted to restricted fluid flow further leading to elevated

crustal temperature (50-100°C within the upper 500 m of the lavas; Alt et al., 2010). The disparate results of these previous studies motivated this work.

Here we use four sections through the 90 Myr Troodos ophiolite that have different hydrological histories to investigate the uptake of Li during low-temperature alteration of the upper oceanic crust. The Troodos ophiolite is the only ophiolite that preserves its seafloor alteration history (e.g. Gillis and Robinson, 1990). For example, unlike most ophiolites, volcanic glass is widely preserved in the Troodos ophiolite (Robinson et al., 1983) and the alteration temperatures in the upper lavas match ocean bottom water temperature (Gillis and Robinson, 1990; Gillis et al., 2015). The common secondary minerals formed during low-temperature alteration of the lava section include smectite, celadonite, zeolites, calcite and K-feldspar with the mineralogy changing with depth in the crust (Gillis and Robinson, 1990). The lavas were buried slowly by sediment, a history typical of much of the abyssal plain but unlike most other ophiolites that, due to forming close to continental margins and/or arc volcanoes, were buried rapidly. We define the uptake flux of Li into the crust under different hydrological conditions and show that most whole-rock Li-isotope compositions of Li-rich samples fall in a narrow range ~10±2‰. We compare the results of this study to published results for samples altered under different conditions. It is concluded that the uptake flux of Li into the upper ocean crust is larger than is generally assumed (and the diagenetic flux likely smaller) and that $\Delta_{SW\text{-}lava}$ probably varies substantially with environmental conditions (e.g. bottom water temperature). These findings have important implications for how paleo-variations in δ^7Li_{SW} should be interpreted.

2. ANALYTICAL METHODS

Bulk rock samples were crushed in an agate planetary mill and major element compositions were determined by XRF at Acme labs, Vancouver. Approximately 100 mg of the bulk-rock powder was dissolved for trace element and Li-isotope analysis in Teflon vials using a standard 10:1 HF:HNO_3 mix on a ~125°C hotplate followed by repeat drying down and digestion in HNO_3 until each sample was fully in solution. Occasional samples that formed precipitates were dried down and digested in HCl then re-dried and taken up in HNO_3. Void-filling celadonite samples (cm-scale) were separated from the rock in the field and, after gentle crushing, sonicated in DI and then hand picked to purify the material. The separates were then crushed by hand and digested in the same way as the bulk-rock samples. Digested rock and celadonite samples were diluted to a mass ratio of approximately 1000-to-1 producing a 2% HNO_3 matrix and then analysed on a Thermo X-Series ICP-MS at the University of Victoria. Indium was added online as the internal standard to correct primary instrumental drift, and a solution made out of aliquots of several samples was run after every six samples as a secondary drift monitor. After internal standardization, drift correction and blank correction (typically <5 ppb), calibration was performed against the standards BIR-1, BHVO-2, BCR-2, JB-2 and JR-2. Reproducibility, based on 14 total procedural duplicates, run over the course of this study, is better than 6.1% for Li concentration in all cases and the average difference between duplicates is 2.3% (Supplementary Table A1).

Samples were selected for Li-isotope analysis so as to investigate variations in isotopic composition with depth in the crust and with location (i.e. hydrological regime) and to build on the data reported by Gillis et al. (2015). We focused on samples with high

Li contents (19-119 ppm) as these are the ones that play the largest role in controlling the isotopic composition of the flux of Li from the ocean into the crust. Additionally, we analysed four large void-filling celadonite separates in order to determine the isotopic composition of celadonite to compare with the bulk-rock compositions. Lithium was separated from the matrix using a standard chromatographic column method based on Tomascak et al. (1999) and described in detail by Brant et al. (2012). Briefly, Teflon columns packed with BIORAD AG50W-X8 (200-400 mesh) resin were conditioned with a nitric-methanol mix prior to loading the samples. Elution was performed using a more concentrated nitric-methanol mix and both a 15 mL aliquot before and after the Li-peak, as well as the Li peak itself, were collected. Analysis of the pre- and post-peak aliquots showed that they contained negligible Li (<3.5 ng and generally <1 ng) as did analysis of total procedural blanks (<0.25 ng and generally <0.1 ng) when compared to the samples (typically >2000 ng).

Samples were analysed on a single collector Thermo X-series ICP-MS at the University of Victoria. Different analytical sessions used slightly different conditions with the majority of samples analysed using a cool plasma set-up but some analysed using a normal (hot) plasma. Cool plasma substantially increases the count rates and hence the precision (e.g. Misra and Froelich, 2009). All solutions were run at ~10 ppb. After tuning the instrument a block of five IRMM-016 solutions were run to define the instrumental drift at the start of the analytical session and then IRMM-016 was run in between every sample. IRMM-016 has a virtually identical Li-isotope ratio to L-SVEC (Jeafcoate et al., 2004) with any difference negligible considering our analytical precision. Each sample and rock standard were analysed five times over the course of an

analytical session with an individual analysis lasting ~250 seconds. The dead time was determined from analysis of a series of solutions with different Li concentrations run at the beginning and end of each analytical session. After dead time correction the isotope ratio for each analysis was determined relative to a polynomial curve fit through the IRMM-016 $^{7}Li/^{6}Li$ data. This approach is similar to standard-sample bracketing but improves the precision of the standard as discussed in detail by Fitzsimmons et al. (2000). Further analytical details are provided in the supplementary materials. The standards BCR-2, BHVO-2, JB-2 and JR-2 were analysed multiple times as part of this study as they span the range of matrix of the unknown samples. Our results are within the range of values reported in the literature (Supplementary Table A4). Four total procedural duplicates (i.e. different rock dissolutions) of the Troodos lavas are all within 1‰ of each other.

Volcanic glass was gently crushed and apparently alteration-free portions were picked under a binocular microscope then mounted in epoxy and polished for analysis. Major elements were determined by electron microprobe at The University of British Columbia using a Cameca SX-50 with a 20 µm beam diameter, 20 nA beam current and 20 kV accelerating voltage. The glass Li concentrations were determined using a New Wave 213 nm laser linked to the same ICP-MS used for solution analysis. A 90 µm spot and 10 Hz repetition rate were used and He was used to transport the ablated material from the laser cell to the ICP-MS. Calibration used Ca as the internal standard (as determined by electron microprobe) and NIST 612 as the single calibration standard. Data quality was checked by analyzing the standards BCR-2G (8.4±0.6 ppm), GOR132-G (9.2±0.9 ppm), KLG-2 (4.9±0.5 ppm) and MLB3 (4.3±0.5 ppm) giving measured

concentrations (in parentheses) that are all within error of the preferred values for these materials.

3. GEOLOGY AND SAMPLE SUITE

Samples used in this study come from a ~20 km east-west section of the northern flank of the Troodos ophiolite that formed in the Cretaceous (~90 Ma; Fig. 2). For the range of plausible half spreading rates of between 1 and 10 cm yr^{-1}, and east-west spreading (in the modern reference frame, given the general north-south dike orientation) this crustal section was built over ~0.2-2 Myr. The Troodos ophiolite formed during a time of high global temperatures on an ice-free world meaning the alteration characteristics in the lavas reflect off-axis fluid-rock reaction under warm bottom-water conditions. Bottom water temperature, based on the minimum temperature determined from oxygen-isotope thermometry using calcite veins and amygdales, was ~10-15°C (e.g. Gillis et al., 2015). Sedimentation rates were low across the entire ophiolite, averaging ≤1 m Myr^{-1} (Bear, 1975), but vary between the study areas.

Four study areas, selected to reflect different paleo-hydrological conditions within the crust, were sampled for whole-rock Li and δ^7Li analysis (Fig. 2). The westernmost section is a paleo-topographic high, that we refer to as the "Mitsero seamount" in which the lava-sediment boundary is ~150 m topographically higher than over most of the study area and, other than patches of umber, the overlying sediments are tens of millions of years younger than elsewhere (Table 1). Umbers occur in several places on top of this paleo-topographic high, and carbonate veins and amygdales are rare in the rocks near the lava-sediment boundary in this area. These observations suggest that this may have been an area of discharge for warm fluids in the off-axis. The easternmost section is a paleo-

topographic low, which we refer to as the "Onophrious graben", in which the lava-sediment boundary is ~50 m topographically lower than over most of the study area; this is believed to have been a site of relatively early sediment accumulation (Bear, 1975; Gillis et al., 2015). The Onophrious section is also dominated by sheet flows; this is hypothesized to have led to lower bulk permeability and reduced fluid flux (Gillis et al., 2015). The other two study areas are in regions with limited variation in seafloor topography and are thought to have "normal" sedimentation histories, intermediate between those of the other sections. One of these is made up of samples from the International Crustal Research Drilling Group drill holes CY1 and CY1a drilled in the Akaki river canyon (Gibson et al., 1991) and the other is a surface transect that we refer to as the "Politico section" (Fig. 2). This range of geological settings will have meant that crustal alteration took place under a range of hydrological conditions and hence had variable fluid-rock reaction histories.

Volcanic glass was sampled throughout the study area and used to define the fresh-rock Li-content. Four large celadonite filled voids were sampled as a way to determine if the celadonite has a similar Li-isotopic composition to the bulk-rocks. No other mineral, except calcite that contains very low Li-contents, could be separated readily in the way celadonite was.

4. RESULTS

4.1. Bulk-rock compositions and the Li-uptake flux

In order to determine the amount of Li taken up during low-temperature alteration of the crust from altered bulk-rock compositions we need to know the initial (fresh) rock Li content. This protolith composition is defined using new laser ablation ICP-MS glass

Li analyses of 80 samples (Supplementary Table A2) in combination with published results from the same area (Regelous et al., 2014; Gillis et al., 2015). Lithium is a moderately incompatible element meaning that the accumulation of phenocrysts (which is generally minor in the Troodos lavas, with the exception of sparse olivine-rich lavas) does not significantly compromise using volcanic glass compositions to define the protolith composition. The Li concentration of volcanic glass increases with differentiation down to an MgO content of ~4 wt% and then decreases (Fig. 3). The decrease in Li content in the most evolved lavas is most simply explained by degassing of a Li-bearing fluid from the magmas (e.g. Kuritani and Nakamura, 2006). Because of this complex behaviour of Li in the more evolved lavas, and the limited change in Li concentration with melt differentiation in the more primitive lavas, it is difficult to use these data to define a protolith composition as a function of the extent of differentiation of the parental melt. Instead we simply take the average measured Li content (4.7 ± 2 ppm; 1σ) as the protolith Li content for all samples.

Bulk-rock Li contents for samples from the four study areas (Fig. 2) are generally strongly enriched in Li with respect to the protolith with Li contents ranging from 3 to 119 ppm with an average of 28 ppm and median of 24 ppm (Fig. 4). There is a general decrease in whole-rock Li content with depth in the crust in each crustal section but with a large scatter at any given depth. The Politico and CY1 sections, which have “typical” sedimentation histories, have quite similar Li contents. The Onophrious graben and Mitsero seamount sections have somewhat lower average Li contents, with strong Li enrichment not extending as deep into the crust as in the Politico and CY1 sections.

These differences likely reflect the different hydrological conditions in different places within the crust (c.f. Gillis et al., 2015).

There is little difference in the Li content of sheet and pillow lavas from the same depth in the crust and, in general, only a slight enrichment of Li in the margins of pillows and sheets relative to their interiors. This indicates that the enrichment of Li in the crust, while heterogeneous, is more strongly a function of depth than lithology. Using the Akaki and Politico sections as the most representative of "normal" altered crust, and fitting the Li content as an exponential function of depth (Fig. 4), leads to an estimated average Li content of the upper 600 m of the crust of 31.8±1.4 ppm (with the uncertainty determined by bootstrapping); i.e. addition of ~27 ppm to the average protolith. Using the measured bulk upper crustal density of 2558±23 kg m^{-3} for lavas in CY1 and 1a, a porosity of 6-18% (Smith and Vine, 1991; Gillis and Sapp, 1997) and an average late-Mesozoic and Cenozoic crustal production rate of 3.4-4.4 km^2 yr^{-1} (Rowley, 2002; Seton et al., 2009), results in an estimated Li uptake flux of 21±2.5 $x10^9$ mol yr^{-1}. Integrating the Li up-take to shallower depths leads to somewhat smaller fluxes (upper 500 m: 19±2.3 $x10^9$ mol yr^{-1}; upper 400m: 18±2.0 $x10^9$ mol yr^{-1}). Alternatively, fitting all of the data in the same manner leads to an average Li content of the upper 600 m of the crust of 23.1±1.1 ppm and a Li flux of 14±2.1 $x10^9$ mol yr^{-1}. These values, which are discussed in more depth below, are significantly larger than have been used in most studies of the global Li-cycle (e.g. $8x10^9$ mol yr^{-1}; Misra and Froelich, 2012).

Bulk-rock Li contents increase with decreasing bulk-rock Na and silicate-Ca (i.e. bulk-rock calcium content corrected for the Ca in calcite calculated assuming all C is in pure $CaCO_3$) and broadly increase with increasing bulk-rock K (Fig. 5). Although these

correlations are scattered it is clear that the bulk-rock Li content acts as a tracer for major element exchange between the fluid and rock. The Troodos lavas extend to more differentiated compositions than is common in normal MORB (including dacites and rare rhyolites; Robinson et al., 1983) allowing some insight into the effect of protolith composition on Li uptake. The Li content of the most evolved bulk-rock samples, with <3.8 wt% MgO and >52wt% SiO_2, are <20 ppm in all except one sample (of ~40). This suggests that these silica-rich, and Mg-poor, protoliths are less susceptible to the formation of Li-rich secondary phases during hydrothermal alteration. However, it should be noted that these samples mainly come from the Onophrious and Mitsero areas where hydrological characteristics may also lead to less Li uptake by the crust.

4.2. Li-isotopes: bulk-rock and celadonite

Whole-rock Li-isotope compositions were measured for samples from each study area to evaluate the isotopic composition of the Li-sink under the varying conditions of alteration experienced in these areas. We focused on samples with relatively high Li-contents as these play the largest role in controlling the bulk Li-isotopic composition of the ocean crust Li-sink. As shown in Figure 1, if the bulk-rock composition is a mixture between a Li-rich altered end-member and the Li-poor protolith, samples are expected to lie along a mixing line in a plot of 1/Li versus δ^7Li (e.g. Chan et al., 1992). For ease of comparison we present the data in the same way in Fig. 6. The initial Li content of the samples defined by the glass data is ~4.7±2 ppm and most likely had a δ^7Li of ~2-5‰ based on comparison with basalt from similar settings (Tomascak et al., 2002; Tomascak et al., 2008).

Most Li-rich samples from all areas, irrespective of the hydrological setting, have similar Li-isotopic composition but samples from the uppermost part of the crust in most sections have slightly lower δ^7Li than samples with similar Li-contents deeper in the crust (Fig. 6 and 7). These isotopically light samples are all from within <40 m of the lava-sediment boundary (Fig. 6 and 7). The sediments immediately overlying the isotopically light samples are umbers in one case and limestone in the other cases suggesting that exchange of Li with pore fluids in the overlying sediment column is unlikely to be the cause of the light Li-isotope signature. Furthermore, in the Mitsero seamount area, other than the thin umber patches, there we no sediments deposited until after alteration of the crust ceased (Table 1). Based on XRD analysis there are no unusual minerals in these samples (K-feldspar, undifferentiated "clay", calcite, magnetite and relic plagioclase). One possible explanation of the isotopically light Li is that beidellite, which is common in K-feldspar-rich samples like these, may have a larger fractionation factor than other Li-rich minerals. This hypothesis is consistent with the observation that the isotopically lightest samples (<0‰) from IODP Hole 1256D are beidellite-rich (Fig. 1; Gao et al., 2012; Alt et al., 2010). Whatever the origin of the isotopically light Li in the uppermost, Li-rich, samples their existence suggests that differences in alteration conditions affect $\Delta_{SW\text{-}lava}$.

Excluding samples from the upper 40 m of the crust, Li-rich samples define a trend of increasing δ^7Li with increasing Li content (Fig. 6b). The Li-rich end of this trend has a δ^7Li of ~10.5±1‰ and the average δ^7Li of the ten samples with >50 ppm Li is 10±0.5‰. Because these samples are dominated by Li added to the crust from seawater this provides an estimate of the δ^7Li of this Li which we conservatively estimate as

10.5±2‰. Two samples with low Li contents (<10 ppm) have much higher δ^7Li than predicted by a simple mixing model between the protolith and an altered end-member. As with the different δ^7Li of the shallowest samples in the crust, this indicates that in detail the alteration process is more complex than simple mixing of an altered end-member with a protolith.

In order to understand the controls on the bulk-isotopic fractionation of Li between seawater and the low-temperature altered ocean crust it is important to understand the role of variations in the mineralogy of the altered crust on its Li-isotope composition. Celadonitic clays in the Troodos lavas can contain >100 ppm Li (Gillis et al., 2015) making them an important Li-sink and, critically, these sometimes fill large voids making it relatively easy to separate this material from the host rock. Because of this four celadonite samples were separated and analysed for their Li content and Li-isotopic composition to determine how closely they matched the altered end-member defined by the whole rock data arrays (Fig. 6). These samples contain 22-33 ppm Li and have δ^7Li between 5.8 and 7.3‰ (Fig. 6; Supplementary Table A3). Three of the separates have trace element compositions very similar to *in situ* analyses of celadonite (Gillis et al., 2015; Brant, 2012) suggesting they are of high purity but one separate was clearly not completely pure celadonite; however, this sample lies in the range of Li and δ^7Li of the other celadonites suggesting that the contaminating material was unimportant to its Li budget. The homogeneous and isotopically light Li-isotopic composition of the celadonites, relative to the altered end-member defined by the whole-rock data, indicates that the celadonite fractionation factor is larger than the bulk fractionation factor. Mass balance thus requires that another alteration phase(s) must be significantly heavier than

404 the whole-rock samples; i.e. different secondary minerals have substantially different Li-
405 isotope fractionation factors. Because which minerals form, and their relative
406 abundances, depends on the alteration conditions this adds support to the suggestion that
407 $\Delta_{SW\text{-}lava}$ is unlikely to be constant at ~16‰ (Fig. 1; Chan et al., 1992; Misra and Froelich,
408 2012). Instead, with changing environmental conditions (e.g. bottom water temperature)
409 the bulk fractionation factor probably varies.

410 **5. DISCUSSION**

411 **5.1. Magnitude and isotopic composition of the Li sink into altered upper oceanic**
412 **crust**

413 In order to quantify the importance of alteration of the upper oceanic crust in off-
414 axis hydrothermal systems for the global Li-cycle we need to know the magnitude and
415 isotopic composition of the Li sink into the upper oceanic crust and how these vary with
416 environmental conditions. Just as it has been hypothesized that the river flux (Vigier and
417 Godderis, 2014) and/or its isotopic composition (Misra and Froelich, 2012) have changed
418 over time due to changing environmental conditions, it is equally likely that the
419 hydrothermal sink into altered upper oceanic crust has changed due to changing
420 environmental conditions. In this section the data reported here for the Troodos ophiolite
421 is compared to previously reported data to investigate the magnitude of the Li-sink and
422 then the controls on $\Delta_{SW\text{-}lava}$.

423 The Li-sink from the ocean into the upper oceanic crust in the late Cretaceous,
424 based on data from the Troodos ophiolite, was between 14±2.1 and 21±2.5 $x10^9$ mol yr^{-1}
425 depending on whether we use all of the data (14±2.1 $x10^9$ mol yr^{-1}) or just data from the
426 study areas with normal sedimentation histories (21±2.5 $x10^9$ mol yr^{-1}). The former is

probably an underestimate as it includes data from the Mitsero seamount and Onophrious graben which are atypical areas that we chose to sample to better understand the role of crustal hydrology in controlling the behaviour of Li. That said, the modern median global abyssal sedimentation rate is higher than that for the Troodos ophiolite (Anderson et al., 2012), meaning that the crust studied here may have interacted with more seawater than typical crust and hence could have accumulated more Li than average ocean crust.

Irrespective of the uncertainties, the Li sink in the Troodos ophiolite appears to have been substantially larger than the Li sink recorded by well-studied drill cores that were much more rapidly sedimented (>20 m Myr^{-1}). The Li content of the upper 600 m of the lavas at Sites 504 and 896 (average 7.5 ppm; n = 18) has been used to estimate a global upper oceanic crust Li sink of ~$2x10^{9}$ mol yr^{-1} (Chan et al., 2002), an order of magnitude smaller than suggested by the Troodos lavas. A slightly lower average Li content of the lavas from Site 1256 (6.4 ppm; n = 92; Gao et al., 2012) suggests a similar uptake flux as at Sites 504 and 896. In contrast, the dredge samples reported by Chan et al. (1992) extend to Li contents as high as 75 ppm, similar to those observed in the Troodos ophiolite. The relatively rapid sedimentation rates for the crust recovered in the drill cores probably means that these sites were altered at smaller fluid fluxes, as well as higher temperatures, than is typical for off-axis hydrothermal systems. These differences probably explain the difference in the calculated Li-sink, although it is also possible that Cretaceous seawater contained more Li and/or that alteration conditions in the Cretaceous led to more efficient Li removal from hydrothermal fluids than is the case today.

Estimating the bulk isotopic fractionation between Cretaceous seawater and Li added to the Troodos upper oceanic crust requires an estimate of the Li-isotopic

composition of the ocean ~70 to 90 Myr ago when alteration occurred (Staudigel et al., 1986; Booij et al., 1995). The only estimate we are aware of comes from Pogge von Strandmann et al. (2013); their data suggest that ~93 Myr seawater had a δ^7Li of ~22±2‰ based on bulk carbonate analyses. Using this value, and the "alteration end-member" of ~10.5‰ (Fig. 6), suggests $\Delta_{SW\text{-}lava}$ was ~11 to 12‰. The bulk Li-isotope fractionation factor is ~3‰ larger for both samples from the very top of the crust (Fig. 7) and for celadonite separates (Fig. 6). This variation in fractionation factor suggests that alteration conditions and/or what phases form during alteration are important in controlling $\Delta_{SW\text{-}lava}$.

The value of $\Delta_{SW\text{-}lava}$ calculated from the Troodos ophiolite of ~11 to 12‰ is considerably smaller than the value determined from dredge samples altered at lower temperatures (~16-17‰; Chan et al., 1992) but somewhat larger than that determined for samples from ODP Sites 504 and 896 (~8 to 10‰; Chan et al., 2002). It is clearly important to understand the origin of this ~7‰ variation in $\Delta_{SW\text{-}lava}$, although with only three study areas that an empirical fractionation factor can be derived from this is difficult to do so unambiguously. We consider two possible models; variation in $\Delta_{SW\text{-}lava}$ due to variable Li loss from a fluid evolving via Rayleigh distillation and variation in $\Delta_{SW\text{-}lava}$ due to variable temperature.

As Li is taken from seawater into minerals in the lavas the fluid is expected to become heavier due to Rayleigh distillation with the extreme end-member of complete removal of Li from the fluid leading to no isotopic fractionation between the fluid and Li added to the crust. Hypothetically removal of variable fractions of the Li from the fluid could lead to variable apparent fractionation factors. However, due to the high water-to-rock ratios in off-axis hydrothermal systems it is unlikely that there is significant Li

depletion in the hydrothermal fluid within the crust. Consideration of the dredge samples, the Troodos samples and the ODP Hole 504B/896A samples support this suggestion as outlined next.

The dredge samples will have been exposed to the ocean throughout their lifetime providing an effectively infinite reservoir of Li to exchange with, thus Rayleigh distillation can be discounted for these samples. The Troodos samples come from sections selected specifically to have had different hydrological histories and hence if Rayleigh distillation was important we would expect to see differences in the "altered end-member" composition in the different areas – the fact this is not observed suggests a minor role for Rayleigh distillation in controlling the isotopic composition of these samples. Finally, the samples from ODP Hole 504B/896A have taken up very little seawater Li (1-3 ppm). To drive a 7‰ difference in $\Delta_{SW\text{-}lava}$ for these samples relative to the dredge samples by Rayleigh distillation would require >60% of the fluid Li to be taken into the rock if at equilibrium the fluid was 16-17‰ heavier than the minerals. Such a high uptake fraction, with little Li added would require unrealistically small water-to-rock ratios (<15). At a more realistic water-to-rock ratio of 500 only 1 to 3% of the Li would have been lost from the hydrothermal fluid leading to a <0.3‰ isotopic shift due to Rayleigh distillation. Furthermore, the Li content of pore fluids in the sediments from around this area approach seawater values as basement is approached suggesting that the basement fluid has a Li content very similar to seawater (Mottl et al., 1983). Similar observations of pore water Li contents converging on seawater Li contents as basement is approach at other sites has been interpreted as indicating large scale replenishment of the crustal aquifer with barely modified seawater (You et al., 2003).

Thus, while some Rayleigh distillation must occur to some extent within the hydrothermal fluid it seems highly unlikely that it dominates the variation in $\Delta_{SW\text{-}lava}$ observed due to the high water-to-rock ratios in off-axis hydrothermal systems.

Our favoured candidate for controlling the observed variation in $\Delta_{SW\text{-}lava}$ is temperature; we note from the start that variation in $\Delta_{SW\text{-}lava}$ with temperature may reflect both thermodynamic controls on isotope partitioning within a single mineral and changes in mineralogy of the altered crust with changing temperature. We estimate alteration temperature for the Troodos ophiolite and drill cores from the average temperature of carbonate mineral precipitation determined from previous O-isotope thermometry (Gillis and Coogan, 2011; Gillis et al., 2015). For the dredge samples the alteration temperature can safely be assumed to match that of bottom water. There is a correlation between the estimated average alteration temperature and $\Delta_{SW\text{-}lava}$ that can be used to define an empirical temperature dependence of $\Delta_{SW\text{-}lava}$ (Fig. 8). This empirically derived temperature dependence is stronger than predicted by extrapolation of the temperature dependence of the Li-isotope fractionation factor determined experimentally for smectite between 90 and 250°C (Fig. 8; Vigier et al., 2008) and the absolute values are quite different to those compiled by Li and West (2014) which included a wide range of mineralogies. These differences should not be surprising given the different minerals involved and we emphasize that the empirical fractionation factor determined here is for alteration of basalt, by seawater, at low temperature. Even in this situation it is likely that the bulk mineralogy (and mineral abundances and compositions) of upper oceanic crust altered under warmer conditions is different than that altered under cool conditions (e.g. Gillis and Coogan, 2011; Coogan and Gillis, 2013). These mineralogical changes in the

519 alteration products may be as important as changes in temperature in controlling $\Delta_{SW\text{-}lava}$.
520 For example, changes in the amount of celadonite in the alteration assemblage will
521 modify the bulk-isotope fractionation factor (Fig. 6).

522 Using the empirical estimate of the temperature dependence of $\Delta_{SW\text{-}lava}$ (Fig. 8)
523 Cenozoic cooling of ocean bottom water by 10-15°C (Lear et al., 2000), which led to a
524 similar decrease in fluid-rock reaction temperatures in off-axis hydrothermal systems
525 (Gillis and Coogan, 2011), may have caused an increase in $\Delta_{SW\text{-}lava}$ of ~3‰. If the entire
526 Li sink from the ocean changed by this much then ~3‰ of the observed ~8‰ increase in
527 seawater δ^7Li would have been driven by this changing sink isotopic composition.

528 **5.2. The oceanic Li cycle**

529 The modern ocean contains ~3.6×10^{16} moles of Li and, based on the Li content of
530 carbonate shells, it appears that there has been relatively little change (±40%) in the Li
531 content of seawater over the last 100 Myr although this is not well constrained (Delaney
532 and Boyle, 1985; Misra and Froelich, 2012). Previous estimates of the flux of Li into the
533 ocean range from ~30 to 40×10^9 mol yr^{-1} (Stoffyn-Egli and Mackenzie, 1984; Seyfried et
534 al., 1984; Misra and Froelich, 2012). These estimates indicate a residence time of Li in
535 the ocean of ~1 Myr although it will be argued below that these fluxes are overestimates
536 and hence the residence time is somewhat longer (but <3 Myr). Given the relatively short
537 residence time of Li in the ocean, changes in the Li-isotopic composition of seawater over
538 multi-million year timescales can be thought of as reflecting changes in the mass balance
539 between the input and output fluxes (Misra and Froelich, 2012; Fig. 1).

540 In the context of the new constraints on the uptake of Li during low-temperature
541 alteration of the upper oceanic crust it is worth considering how robust the constraints on

542 the other primary fluxes controlling the Li cycle in the ocean are (Fig. 1). In addition to
543 uptake of Li during low-temperature alteration of the upper crust, the other major output
544 flux of Li from the ocean is thought to be diagenesis of marine sediments. The diagenetic
545 flux of Li from the ocean has been estimated at ~20 to $28x10^9$ mol yr^{-1} based on the
546 difference in composition between average continental igneous rocks and marine clays
547 (Misra and Froelich, 2012; Seyfried et al., 1984). This approach is complicated by
548 uncertainties in both the pre-diagenesis sediment composition and the fractions of low Li
549 'sand' versus high Li 'clay' derived from weathering. For example, estimates of the Li
550 content of upper continental crust range from ~20 ppm (Taylor and Mclennan, 1995) to
551 35±11 ppm (Teng et al., 2004) leading to substantial uncertainties in any estimate of a
552 flux based on the difference in composition of average marine clays and upper
553 continental crust. Further, a substantial difference in Li content (10's of ppm) between the
554 suspended and bed load in rivers has been reported (Kisakürek et al., 2005) indicating
555 that part of the difference in Li content between marine clays and upper continental crust
556 may be generated before delivery of the clay to the ocean rather than during diagenesis.
557 Pore fluids within marine sediments also provide insight into diagenetic fluxes. These can
558 be both enriched and depleted in Li and have heavier or lighter isotopic compositions
559 (e.g. Stoffyn-Egli and Mackenzie, 1984; You et al., 1995; Zhang et al., 1998; James and
560 Palmer, 2000; You et al., 2003). The average Li content of pore fluids in ODP sediment
561 cores in the compilation of Scholz et al. (2010; their supplementary material) is 77±141
562 µmol L^{-1} (median 20 µmol L^{-1}) almost three times the seawater Li content (26 µmol L^{-1})
563 but with very large uncertainties. Taken at face value these pore fluid data suggest that
564 there is a flux of Li from marine sediments into the ocean not the reverse (Stoffyn-Egli

565 and Mackenzie, 1984). However, in many locations the Li content of pore fluid is
566 enriched relative to seawater deep in the sediment pile and depleted closer to the
567 sediment-water interface. It is beyond the scope of this study to derive a new estimate of
568 the Li flux associated with marine sediment diagenesis and we simply note that the
569 diagentic Li flux is poorly constrained.

570 The major input fluxes of Li to the ocean are high-temperature hydrothermal
571 systems and rivers. Early estimates of the Li flux associated with high-temperature
572 hydrothermal systems were largely based on measured vent fluid compositions and were
573 very large (15-27x10^9 mol yr^{-1}; Stoffyn-Egli and Mackenzie, 1984; Seyfried et al., 1984)
574 and a similarly large value was used by Misra and Froelich (13x10^9 mol yr^{-1}; 2012).
575 Given an average MORB Li content of 6 ppm (Gale et al., 2013), leaching of all of the Li
576 from 1000 m thickness of sheeted dikes (which are the source of most Li leached from
577 the crust), over the area of new crust produced annually (3.4 km^2) would give a Li flux of
578 6.6 x10^9 mol yr^{-1}. This back-of-the-envelope calculation demonstrates that these
579 estimates are all likely to be substantial over-estimates of the Li flux from high-
580 temperature hydrothermal systems. Indeed, the high-temperature hydrothermal Li flux
581 has recently been re-evaluated using the compositions of both vent fluids and sheeted
582 dikes, in combination with the fluxes of many other elements leading to a considerably
583 smaller, and far better constrained, flux (5.2±1.4x10^9 mol yr^{-1}, 6.3±0.7‰; Coogan and
584 Dosso, 2012).

585 A modern river Li flux of 8x10^9 mol yr^{-1}, with a δ^7Li of 23‰, was estimated by
586 Huh et al. (1998) and an updated flux of 10x10^9 mol yr^{-1} from Gaillardet et al. (2014), at
587 the same isotopic composition, was used by Misra and Froelich (2012). This value may

588 be an upper limit on the steady-state river flux given both the possibility of significant Li
589 removal in estuaries (Pogge von Strandmann et al., 2008) and uncertainty in the role of
590 agriculture (especially fertilizers) in modifying the Li content (and isotopic composition)
591 of modern rivers (e.g. Kisakürek et al., 2005; Clergue et al., 2015). There is an apparent
592 decrease in δ^7Li of the dissolved load with increasing chemical weathering rate
593 (Kisakürek et al., 2005; Pogge von Strandmann et al., 2006; Vigier et al., 2009) but there
594 are large uncertainties in how much the riverine Li-flux and/or its isotopic composition
595 has changed over time.

596 In summary, our best estimates of the modern input flux of Li to the ocean is ~12-
597 17x10^9 mol yr^{-1} (5.2±1.4x10^9 + 8 to 10x10^9 mol yr^{-1}) giving a residence time of 2 to 3
598 Myr. If the ocean is at steady-state, and the river and high-temperature hydrothermal
599 fluxes are 5.2x10^9 and 10x10^9 mol yr^{-1} with δ^7Li of 23‰ and 6.3‰ respectively, then the
600 modern bulk Li sink from the ocean must be 13.5% lighter than seawater; this value has
601 significant uncertainty. The magnitude of the Li sink in the Troodos upper crust estimated
602 here (14 to 21x10^9 mol yr^{-1}) overlaps with the modern Li sources to the ocean suggesting
603 that low-temperature alteration of the upper oceanic crust in off-axis hydrothermal
604 systems may be the main sink of Li from the ocean; i.e. there is no requirement for there
605 to be a large diagenetic Li sink. However, it is possible that the magnitude of the Li
606 sources and sinks have changed over time and these may have been larger in the late
607 Cretaceous.

608 **5.3. Linking the Li- and C-cycles**

609 The publication of a high fidelity Li-isotope record for seawater (Misra and
610 Froelich, 2012) has inspired significant interest in trying to use this to understand the

long-term carbon cycle (e.g. Misra and Froelich, 2012; Li and West, 2014; Wanner et al., 2014; Vigier and Godderis, 2014; Liu et al., 2015). On a million year timescale there has to be a balance in the flux of carbon between the solid earth and the ocean-atmosphere system to avoid massive changes in atmospheric CO_2 levels and hence Earth's climate (e.g. Berner and Caldeira, 1997). Two commonly discussed drivers of changes in atmospheric CO_2 levels are changes in the degassing rate of CO_2 from the solid earth and changes in the weatherability of the continents.

If the CO_2 degassing rate is the primary driver of changes in the CO_2 inventory in the ocean-atmosphere system then it is commonly assumed that this scales with the rate of creation of new oceanic crust. In this scenario, decreased CO_2 degassing would correlate with a decreased high-temperature hydrothermal flux leading to a smaller input of isotopically light Li at high-temperature vents and hence increased δ^7Li_{SW}. For example, a 20% decrease in the high-temperature hydrothermal flux would lead to ~1‰ increase in δ^7Li_{SW} assuming that both the river flux, and the isotopic fractionation between the bulk Li sink and the ocean, remained constant but that the Li sink decreased in magnitude to match the input sources; this is a relatively small, but not negligible, effect. However, decreased CO_2 degassing would lead to a lower steady-state atmospheric CO_2 content and hence a cooler climate, all other things being equal. In turn this would lead to the average temperature of fluid in off-axis hydrothermal systems being cooler, and thus $\Delta_{SW\text{-}lava}$ would increase (Fig. 8, 9). Using the empirically derived temperature dependence of $\Delta_{SW\text{-}lava}$ (Fig. 8) cooling of bottom water by 10-15°C would lead to an increase in $\Delta_{SW\text{-}lava}$ of 2 to 3‰ driving the isotopic composition of seawater higher. Combined with the decreased high-temperature hydrothermal flux, this could

explain between a third and a half of the change in δ^7Li_{SW} over the Cenozoic. In the alternative model, in which steady-state atmospheric CO_2 levels decrease due to increased weatherability of the continents, for example due to mountain building (e.g. Raymo and Ruddiman, 1992), cooling would occur without a decreased hydrothermal flux. Thus, the increase in δ^7Li_{SW} due to interaction between the ocean and seafloor would be ~1‰ smaller.

The ~9‰ increase in δ^7Li_{SW} over the Cenozoic (Misra and Froelich, 2012) would appear to require changes in the river Li flux and/or river Li-isotopic composition in addition to changes in the seafloor hydrothermal fluxes discussed above. However, exactly what this would be is debated with models ranging from massive (~20‰), to large (~13‰), to no changes in δ^7Li_{riv} (respectively, Misra and Froelich, 2012; Li and West, 2014; Vigier and Godderis, 2014) and no (Misra and Froelich, 2012) to massive (Vigier and Godderis, 2014) changes in the river Li flux. The trade-off between changes in the river and high-temperature hydrothermal fluxes and the river δ^7Li required to explain the δ^7Li_{SW} low of 22‰ is shown in Figure 9. At modern river and high-temperature hydrothermal fluxes, and a 3‰ smaller fractionation between seawater and the oceanic Li sink than is required for the modern system to be at steady-state, a river δ^7Li of ~14‰ is required. However, the riverine flux does not have to have been this isotopically light if either the river flux was smaller (Vigier and Godderis, 2014) or the high-temperature hydrothermal flux was larger (Fig. 9).

6. SUMMARY AND CONCLUSIONS

We studied four sections through the lava pile of the Troodos ophiolite to determine the magnitude and isotopic composition of the Li-sink into the upper oceanic crust during low-temperature off-axis hydrothermal circulation. The hydrological conditions within the crust, controlled by paleo-seafloor topography, play a significant role in controlling the Li uptake flux. Comparison of the uptake flux from the Troodos ophiolite, with previous estimates from drill cores recovered from regions of anomalous sedimentation history, indicate that the magnitude of the Li-uptake flux has previously been under-estimated. Indeed, the Li-uptake flux in the Troodos ophiolite (14 to 21×10^9 mol yr^{-1}) overlaps estimates of the flux of Li into the ocean from rivers and on-axis high-temperature hydrothermal systems (12 to 17×10^9 mol yr^{-1}) suggesting alteration of the upper oceanic crust is the dominant Li-sink from the ocean.

The Li-isotopic composition of altered upper crust from the Troodos ophiolite that has taken up a large amount of seawater Li (~10±2‰) is ~11 to 12‰ lighter than contemporaneous seawater. Comparison of this empirically derived fractionation factor with that from a series of dredge samples (Chan et al., 1992) and samples from ODP Sites 504B and 896A (Chan et al., 2002) allows an empirical temperature dependence of the fractionation factor to be derived (Fig. 8). Temperature, however, is not the only control on the Li-isotopic composition of altered upper oceanic crust. Samples from the uppermost portion of the crust are isotopic lighter than deeper samples. Additionally, celadonite separates are isotopically lighter than bulk-rock samples; mass balance requires other phases to be isotopically heavier than the bulk rock. These observations are interpreted to indicate that the isotopic fractionation between the altered oceanic crust and

secondary minerals is not simply controlled by a direct temperature-dependence of the isotopic fractionation factor but also by less direct dependence of the alteration assemblage on the overall alteration conditions.

The new data presented here, along with the use of better estimates of the high-temperature hydrothermal flux, allows a re-evaluation of the changes in the global Li cycle required to drive the change in δ^7Li_{SW} over the Cenozoic. If we are correct that cooling bottom water will have increased $\Delta_{SW\text{-}lava}$ by ~3‰ over the Cenozoic, then a combination of a slightly larger high-temperature hydrothermal flux and a modest decrease in either the Li-isotopic composition of, or Li-flux from, rivers could explain the much lighter Li-isotopic composition of early Cenozoic seawater (Fig. 9).

ACKNOWLEDGEMENT

We thank Sambuddha Misra and two anonymous reviewers for their input that helped improve the manuscript as well as Aerona Moore for field and lab assistance, Mina Seyedali for discussion and Mati Raudsepp and his team for XRD analysis and assistance with electron microprobe analysis. LAC and KMG were funded through NSERC Discovery (5098 & 155396) and Accelerator grants.

REFERENCES

Alt J. C., Laverne C., Coggon R. M., Teagle D. A. H., Banerjee N. R., Morgan S., Smith-Duque C. E., Harris M. and Galli L. (2010) Subsurface structure of a submarine hydrothermal system in ocean crust formed at the East Pacific Rise, ODP/IODP Site 1256. *Geochemistry Geophys. Geosystems* **11**, doi:10.1029/2010GC003144.

699 Anderson B. W., Coogan L. A. and Gillis K. M. (2012) The role of outcrop-to-outcrop
700 fluid flow in off-axis oceanic hydrothermal systems under abyssal sedimentation
701 conditions. *J. Geophys. Res.* **117**, doi:10.1029/2011JB009052.
702 Bear, L.M., 1975. The geology and mineral resources of the Akaki-Lythrodondha area
703 (2nd Edition). Cyprus Geological Survey Department Memoir 3. Government of
704 Cyprus, Nicosia, 122 pp.
705 Berner R. A. and Caldeira K. (1997) The need for mass balance and feedback in the
706 geochemical carbon cycle. *Geology* **25**, 955–956.
707 Bickle M. J., Harris N. B. W., Bunbury J. M., Chapman H. J., Fairchild I. J. and Ahmad
708 T. (2001) Controls on the 87Sr/86Sr ratio of carbonates in the Garhwal Himalaya,
709 headwaters of the Ganges. *J. Geol.* **109**, 737–753.
710 Booij E., Gallahan W. E. and Staudigel H. (1995) Ion-exchange experiments and Rb/Sr
711 dating on celadonites from the Troodos ophiolite, Cyprus. *Chem. Geol.* **126**, 155–
712 167.
713 Brady P. V and Gislason S. R. (1997) Seafloor weathering controls on atmospheric CO2
714 and global climate. *Geochim. Cosmochim. Acta* **61**, 965–973.
715 Brant C., Coogan L. A., Gillis K. M., Seyfried W. E., Pester N. J. and Spence J. Lithium
716 and Li-isotopes in young altered upper oceanic crust from the East Pacific Rise.
717 *Geochim. Cosmochim. Acta* **96**, 272-293.
718 Chan L. H., Edmond J. M., Thompson G. and Gillis K. (1992) Lithium isotopic
719 composition of submarine basalts: implications for the lithium cycle in the oceans.
720 *Earth Planet. Sci. Lett.* **108**, 151–160.

721 Chan L.-H., Alt J. C. and Teagle D. A. H. (2002) Lithium and lithium isotope profiles
722 through the upper oceanic crust: a study of seawater-basalt exchange at ODP Sites
723 504B and 896A. *Earth Planet. Sci. Lett.* **201**, 187–201.
724 Clergue C., Dellinger M., Buss H. L., Gaillardet J., Benedetti M. F. and Dessert C. (2015)
725 Influence of atmospheric deposits and secondary minerals on Li isotopes budget in a
726 highly weathered catchment, Guadeloupe (Lesser Antilles). *Chem. Geol.* **414**, 28–
727 41.
728 Coogan L. A. and Dosso S. (2012) An internally consistent, probabilistic, determination
729 of ridge-axis hydrothermal fluxes from basalt-hosted systems. *Earth Planet. Sci.*
730 *Lett.* **323**, 92–101.
731 Coogan L. A. and Dosso S. E. (2015) Alteration of ocean crust provides a strong
732 temperature dependent feedback on the geological carbon cycle and is a primary
733 driver of the Sr-isotopic composition of seawater. *Earth Planet. Sci. Lett.* **415**, 38–
734 46.
735 Coogan L. A. and Gillis K. M. (2013) Evidence that low-temperature oceanic
736 hydrothermal systems play an important role in the silicate-carbonate weathering
737 cycle and long-term climate regulation. *Geochemistry, Geophys. Geosystems* **14**,
738 1771–1786.
739 Delaney M. L. and Boyle E. A. (1985) Lithium in foraminiferal shells: implications for
740 high-temperature hydrothermal circulation fluxes and oceanic crustal generation
741 rates. *Earth Planet. Sci. Lett.* **80**, 91–105.
742 Edmond J. M. (1992) Himalayan tectonics, weathering processes, and the strontium
743 isotope record in marine limestones. *Science* **258**, 1594–1597.

744 Fisher A. T. (2005) Marine hydrogeology: recent accomplishments and future
745 opportunities. *Hydrogeol. J.* **13**, 69–97.
746 Fisher A. T. and Wheat C. G. (2010) Seamounts as Conduits for Massive Fluid, Heat, and
747 Solute Fluxes on Ridge Flanks. Oceanography **23**, 74–87.
748 Fitzsimons I. C. W., Harte B. and Clark R. M. (2000) Sims stable isotope measurement:
749 counting statistics and analytical precision. *Min. Mag*. **64**, 59–83.
750 Gaillardet J., Dupre B., Louvat P. and Allegre C. J. (1999) Global silicate weathering and
751 CO2 consumption rates deduced from the chemistry of large rivers. *Chem. Geol.*
752 **159**, 3–30.
753 Gaillardet J., Viers J. and Dupré B. (2014) Trace Elements in River Waters, in Treatise
754 on Geochemistry (2nd Ed) Editor Holland, Heinrich D. and Turekian, K. Elsevier,
755 Oxford. pp. 195–235.
756 Gale A., Dalton C. A., Langmuir C. H., Su Y. and Schilling J. G. (2013) The mean
757 composition of ocean ridge basalts. *Geochemistry, Geophys. Geosystems* **14**, 489–
758 518.
759 Gao Y., Vils F., Cooper K. M., Banerjee N., Harris M., Hoefs J., Teagle D. A. H., Casey
760 J. F., Elliott T., Laverne C., Alt J. C. and Muehlenbachs K. (2012) Downhole
761 variation of lithium and oxygen isotopic compositions of oceanic crust at East
762 Pacific Rise, ODP Site 1256. *Geochemistry, Geophys. Geosystems* **13**,
763 Gibson I. L., Malpas J., Robinson P. T. and Xenophontos C. (1991) *Cyprus crustal study*
764 *project: initial report, Hole CY-1 and 1a*., Geological Survey of Canada paper 90-
765 20.

766 Gillis K. M. and Robinson P. T. (1988) Distribution of alteration zones in the upper
767 oceanic crust. *Geology* **16**, 262–266.
768 Gillis K. M. and Robinson P. T. (1990) Patterns and processes of alteration in the lavas
769 and dykes of the Troodos Ophiolite, Cyprus. *J. Geophys. Res.* **95**, 21,521–523,548.
770 Gillis K. M. and Coogan L. A. (2011) Secular variation in carbon uptake into the ocean
771 crust. *Earth Planet. Sci. Lett.* **302**, 385–392.
772 Gillis K. M., Coogan L. A. and Brant C. (2015) The role of sedimentation history and
773 lithology on fluid flow and reactions in off-axis hydrothermal systems: A
774 perspective from the Troodos ophiolite. *Chem. Geol.* **414**, 84–94.
775 Hathorne E. C. and James R. H. (2006) Temporal record of lithium in seawater: A tracer
776 for silicate weathering? *Earth Planet. Sci. Lett.* **246**, 393–406.
777 Higgins J. A. and Schrag D. P. (2015) The Mg isotopic composition of Cenozoic
778 seawater – evidence for a link between Mg-clays, seawater Mg/Ca, and climate.
779 *Earth Planet. Sci. Lett.* **416**, 73–81.
780 Huh Y., Chan L.-H., Zhang L. and Edmond J. M. (1998) Lithium and its isotopes in
781 major world rivers: implications for weathering and the oceanic budget. *Geochim.*
782 *Cosmochim. Acta* **62**, 2039–2051.
783 James R. H. and Palmer M. R. (2000) Marine geochemical cycles of the alkali elements
784 and boron: The role of sediments. *Geochemica Cosmochim Acta* **64**, 3111–3122.
785 Jeffcoate A. B., Elliott T., Thomas A. and Bouman C. (2004) Precise, small sample size
786 determinations of lithium isotopic compositions of geological reference materials and
787 modern seawater by MC-ICP-MS. Geostand. Geoanalytical Res. 28, 161–172.

788 Kisakurek B., James R. H. and Harris N. B. W. (2005) Li and delta Li-7 in Himalayan
789 rivers: Proxies for silicate weathering? *Earth Planet. Sci. Lett.* **237**, 387–401.
790 Kump L. R., Brantley S. L. and Arthur M. A. (2000) Chemical, weathering, atmospheric
791 CO2, and climate. *Annu. Rev. Earth Planet. Sci.* **28**, 611–667.
792 Kuritani T. and Nakamura E. (2006) Elemental fractionation in lavas during post-eruptive
793 degassing: Evidence from trachytic lavas, Rishiri Volcano, Japan. J. Volcanol.
794 Geotherm. Res. 149, 124–138.
795 Li G. and West A. J. (2014) Evolution of Cenozoic seawater lithium isotopes: Coupling
796 of global denudation regime and shifting seawater sinks. *Earth Planet. Sci. Lett.* **401**,
797 284–293.
798 Li G., Hartmann J., Derry L. A., West A. J., You C.-F., Long X., Zhan T., Li L., Li G.,
799 Qiu W., Li T., Liu L., Chen Y., Ji J., Zhao L. and Chen J. (2016) Temperature
800 dependence of basalt weathering. *Earth Planet. Sci. Lett.* **443**, 59–69.
801 Liu X.-M., Wanner C., Rudnick R. L. and McDonough W. F. (2015) Processes
802 controlling δ7Li in rivers illuminated by study of streams and groundwaters draining
803 basalts. *Earth Planet. Sci. Lett.* **409**, 212–224.
804 Mills B., Daines S. J. and Lenton T. M. (2014) Changing tectonic controls on the long-
805 term carbon cycle from Mesozoic to present. *Geochemistry, Geophys. Geosystems*
806 **15**, 4866–4884.
807 Misra S. and Froelich P. N. (2012) Lithium Isotope History of Cenozoic Seawater:
808 Changes in Silicate Weathering and Reverse Weathering. *Science* **335**, 818–823.

809 Misra S. and Froelich P. N. (2009) Measurement of lithium isotope ratios by quadrupole-
810 ICP-MS: application to seawater and natural carbonates. *J. Anal. At. Spectrom.* **24**,
811 1524–1533.
812 Mottl M. J., Lawrence J. R. and Keigwin L. D. (1983) Elemental and stable isotope
813 composition of pore waters and carbonate sediments from deep sea drilling project
814 sites 501/504 and 505. In *Initial Reports DSDP 69* pp. 461–473.
815 Pogge von Strandmann P. A. E., Burton K. W., James R. H., van Calsteren P., Gislason
816 S. R. and Mokadem F. (2006) Riverine behaviour of uranium and lithium isotopes in
817 an actively glaciated basaltic terrain. *Earth Planet Sci. Lett.* **251**, 134–147.
818 Pogge von Strandmann P. A. E., James R. H., van Calsteren P., Gislason S. R. and
819 Burton K. W. (2008) Lithium, magnesium and uranium isotope behaviour in the
820 estuarine environment of basaltic islands. *Earth Planet. Sci. Lett.* **274**, 462–471.
821 Pogge von Strandmann P. A. E., Jenkyns H. C. and Woodfine R. G. (2013) Lithium
822 isotope evidence for enhanced weathering during Oceanic Anoxic Event 2. *Nat.*
823 *Geosci.* **6**, 668–672.
824 Raymo M. E. and Ruddiman W. F. (1992) Tectonic forcing of late Cenozoic climate.
825 *Nature* **359**, 117–122.
826 Regelous M., Haase K. M., Freund S., Keith M., Weinzierl C. G., Beier C., Brandl P. A.,
827 Endres T. and Schmidt H. (2014) Formation of the Troodos Ophiolite at a triple
828 junction: Evidence from trace elements in volcanic glass. *Chem. Geol.* **386**, 66–79.
829 Robinson P. T., Melson W. G., O'Hearn T. and Schmincke H.-U. (1983) Volcanic glass
830 compositions of the Troodos ophiolite, Cyprus. *Geology* **11**, 400–404.

831 Rowley D. B. (2002) Rate of plate creation and destruction: 180 Ma to present. *Geol.*
832 *Surv. Am. Bull.* **114**, 927–933.
833 Scholz F., Hensen C., De Lange G. J., Haeckel M., Liebetrau V., Meixner A., Reitz A.
834 and Romer R. L. (2010) Lithium isotope geochemistry of marine pore waters –
835 Insights from cold seep fluids. *Geochim. Cosmochim. Acta* **74**, 3459–3475.
836 Seton M., Gaina C., Muller R. D. and Heine C. (2009) Mid-Cretaceous seafloor
837 spreading pulse: Fact or fiction? Geology 37, 687–690.
838 Seyfried Jr. W. E., Janecky D. R. and Mottl M. J. (1984) Alteration of the oceanic crust:
839 implications for geochemical cycles of lithium and boron. *Geochim. Cosmochim.*
840 *Acta* **48**, 557–569.
841 Smith and Vine (1991) The physical properties of basalts from CCSP drillholes CY1 and
842 CY1A, Akaki canyon, Cyprus; in Cyprus crustal drilling project: initial report, Hole
843 CY1 and 1A, eds. Gibson, I.L., Malpas, J., Robinson, P.T., and Xenophontos, C;
844 Geological Survey of Canada, Paper 90-20, p 219-234.
845 Spinelli G. A., Giambalvo E. R. and Fisher A. T. (2004) Sediment permeability,
846 distribution, and influence on fluxes in oceanic basement. In Hydrogeology of the
847 Oceanic Lithosphere (eds. E. Davis and H. Elderfield). Cambridge University Press.
848 p. 151–188.
849 Staudigel H., Gillis K. and Duncan R. (1986) K/Ar and Rb/Sr ages of celadonites from
850 the Troodos ophiolite, Cyprus. *Geology* **14**, 72–75.
851 Stoffyn-Egli P. and Mackenzie F. T. (1984) Mass balance of dissolved lithium in the
852 oceans. *Geochim. Cosmochim. Acta* **48**, 859–872.

853 Taylor S. R. and McLennan S. M. (1995) The geochemical evolution of the continental
854 crust. *Rev. Geophys.* **33**, 241–265.
855 Teng F. Z., McDonough W. F., Rudnick R. L., Dalpe C., Tomascak P. B., Chappell B.
856 W. and Gao S. (2004) Lithium isotopic composition and concentration of the upper
857 continental crust. *Geochim. Cosmochim. Acta* **68**, 4167–4178.
858 Tomascak P. B., Carlson R. W. and Shirey S. B. (1999) Accurate and precise
859 determination of Li isotopic compositions by multi-collector sector ICP-MS. *Chem.*
860 *Geol.* **158**, 145–154.
861 Tomascak P. B., Langmuir C. H., le Roux P. J. and Shirey S. B. (2008) Lithium isotopes
862 in global mid-ocean ridge basalts. *Geochim. Cosmochim. Acta* **72**, 1626–1637.
863 Tomascak P. B., Widom E., Benton L. D., Goldstein S. L. and Ryan J. G. (2002) The
864 control of lithium budgets in island arcs. *Earth Planet. Sci. Lett.* **196**, 227–238.
865 Vigier N., Decarreau A., Millot R., Carignan J., Petit S. and France-Lanord C. (2008)
866 Quantifying Li isotope fractionation during smectite formation and implications for
867 the Li cycle. *Geochim. Cosmochim. Acta* **72**, 780–792.
868 Vigier N., Gislason S. R., Burton K. W., Millot R. and Mokadem F. (2009) The
869 relationship between riverine lithium isotope composition and silicate weathering
870 rates in Iceland. *Earth Planet. Sci. Lett.* **287**, 434–441.
871 Vigier N. and Goddéris Y. (2015) A new approach for modeling Cenozoic oceanic
872 lithium isotope paleo-variations: the key role of climate. *Clim. Past* **11**, 635–645.
873 Walker J. C. G., Hays P. B. and Kasting J. F. (1981) A negative feedback mechanism for
874 the long-term stabilization of Earths surface temperature. *J. Geophys. Res.* **86**, 9776–
875 9782.

Wanner C., Sonnenthal E. L. and Liu X.-M. (2014) Seawater δ^7Li: A direct proxy for global CO2 consumption by continental silicate weathering? *Chem. Geol.* **381**, 154–167.

West A. J., Galy A. and Bickle M. (2005) Tectonic and climatic controls on silicate weathering. *Earth Planet. Sci. Lett.* **235**, 211–228.

White A. F. and Buss H. L. (2014) Natural Weathering Rates of Silicate Minerals, in Treatise on Geochemistry (2nd Ed) Editor Holland, Heinrich D. and Turekian, K. Elsevier, Oxford. pp. 115–155.

You C. F., Chan L. H., Gieskes J. M. and Klinkhammer G. P. (2003) Seawater intrusion through the oceanic crust and carbonate sediment in the Equatorial Pacific: Lithium abundance and isotopic evidence. *Geophys. Res. Lett.* **30**.

You C. F., Chan L. H., Spivack A. J. and Gieskes J. M. (1995) Lithium, boron, and their isotopes in sediments and pore waters of ocean drilling program Site 808, Nankai trough – implications for fluid expulsion in accretionary prisms. *Geology* **23**, 37–40.

Zhang L. B., Chan L. H. and Gieskes J. M. (1998) Lithium isotope geochemistry of pore waters from Ocean Drilling Program Sites 918 and 919, Irminger Basin. *Geochemica Cosmochim Acta* **62**, 2437–2450.

FIGURE CAPTIONS

Figure 1. (a) Cartoon of the global Li cycle showing the large ranges of previously published values for the average fluxes and isotopic compositions for the main oceanic sources and sinks of Li. While some of the variation must be real, driving changes in

899 seawater Li compositions, there are also large gaps in our understanding of the Li-cycle
900 inhibiting use of the record of seawater δ^7Li to interpret paleo-enviromental change. OC:
901 fresh oceanic crust; UCC: upper continental crust; (b) Li-isotopic composition of low-
902 temperature lavas that have taken up seawater Li plotted against the reciprocal of their Li
903 content. Only lavas from the upper 500 m of the crust with >4 ppm Li are shown. The
904 data for dredge samples (<10 Myr samples are shown as small symbols and >30 Myr
905 samples as large symbols) and the adjacent ODP Sites 504 and 896 can be explained by
906 mixing between a fresh rock and a high Li alteration component added from seawater as
907 shown by the regression lines. However, the isotopic composition of this end-member
908 appears to be different in each location suggesting there may be significant variation in
909 $\Delta_{SW\text{-}lava}$. Such a mixing trend is not clear in the data from IODP Site 1256. Sources of
910 data: Stoffyn-Egli and Mackenzie (1984); Seyfried et al. (1984); Chan et al. (1992); Huh
911 et al. (1998); Chan et al. (2002); Teng et al. (2004); Tomascak et al. (2008); Coogan and
912 Dosso (2012); Gao et al. (2012); Misra and Froelich (2012) and Li and West (2014).
913
914 Figure 2. Map showing the distribution of samples used in this study within the lava
915 section of the Troodos ophiolite. The inset map shows the location of the study area
916 within Cyprus in the eastern Mediterranean. Red text gives the names of the sections in
917 which whole-rock samples were collected and black text are names of villages.
918 Coordinate system is WGS84 throughout except inset map shows latitude and longitude
919 in degrees. Whole-rock samples from the Akaki Canyon are from drill cores and other
920 samples are from surface outcrops – we see no difference in composition between core
921 and surface samples.

Figure 3. Variation of Li concentration with differentiation, traced by MgO content, in the Troodos volcanic glasses. The general increase in Li with differentiation, then decrease in the most evolved samples, is outlined by the grey field and is interpreted to reflect Li behaving incompatibly until the more evolved magmas started degassing a hydrous fluid which Li partitioned into. Four glasses have Li contents >10 ppm and are indicated by arrows at their respective MgO content. Black symbols are data from our group (this study and Gillis et al., 2015) and grey symbols are from Regelous et al. (2014). The black square with error bars is the average and one standard deviation of the glass dataset as discussed in the text.

Figure 4. Bulk-rock Li concentration as a function of depth in the crust in the four sections studied from west (left) to east (right). An exponential fit through the data from the "normal" Akaki and Politico sections is shown ($Li = 69.2Exp[-3.044x10^{-3}depth]$). Grey symbols are all of the data shown for comparison.

Figure 5. Cross plots of bulk-rock compositions showing broad correlations between increasing Li and: (a) decreasing silicate CaO (defined as $CaO-1.27xCO_2$); (b) decreasing Na_2O and (c) increasing K_2O. These data suggest that Li uptake correlates with the exchange of major elements between the crust and hydrothermal fluid. The black polygon shows the field of volcanic glasses excluding the four shown by arrows in Fig. 3.

Figure 6. (a) Whole-rock and celadonite Li-isotope compositions plotted against 1/Li. Most Li-rich samples have δ^7Li of 9.5±2.5‰ (red dashed polygon) irrespective of which area they come from. The only whole rock samples with as light Li-isotopic compositions as the celadonites (purple polygon) are from the upper 40 m (shown by grey rims) and are not rich in celadonite; see text for discussion. The grey box shows likely protolith compositions. (b) as part (a) but excluding the celadonite samples and samples from the upper 40 m of the crust for clarity.

Figure 7. Bulk-rock Li-isotope compositions as a function of depth in the crust in the four sections studied from west (left) to east (right). Grey symbols are all of the data for samples containing >25 ppm Li (i.e. for which the Li-isotope composition is overwhelmingly controlled by the seawater Li added) shown for comparison. The samples from the Onophrious section that contain <15 ppm Li are labeled with their Li content. See text for discussion.

Figure 8. Comparison of the empirically determined temperature dependence of the Li-isotope fractionation factor between the alteration products in the upper oceanic crust and seawater (red symbols and regression line) with the experimentally determined temperature dependence for smectite (Vigier et al., 2008; blue line). The latter excludes experiments at <90°C which may not give values applicable to nature due to low crystallinity (Vigier et al., 2008). The alteration temperature for the empirical calibration is determined for the middle of the lava pile by regression of alteration temperature

966 (determined from carbonate O-isotope thermometry) versus depth for the Troodos and
967 504/896 datasets. For the dredge samples a seafloor temperature of 4±2°C is assumed.
968
969 Figure 9. Results of a steady-state model for the Li-isotopic composition of seawater
970 (using Eq. 3 of Vigier and Godderis, 2014) for an ocean with δ^7Li_{SW} = 22‰ (early
971 Cenozoic; Misra and Froelich, 2012). The isotopic composition of the high-temperature
972 hydrothermal flux is 6.3‰ and the Li sink from the ocean is 10.5‰. This is 3‰ smaller
973 than the value required for the modern ocean to be at steady-state (13.5‰) given the
974 assumed fluxes (see text for discussion). Assuming modern river and high-temperature
975 hydrothermal fluxes of Li (M on figure), such a light isotopic composition of Cretaceous
976 seawater requires the average river flux of Li to have been isotopically very light
977 (~14‰). However, the average Li delivered to the ocean from rivers may have been
978 significantly heavier if the hydrothermal Li flux was larger and/or the river Li flux was
979 smaller.
980

981

982 **TABLES**

983

984 Table 1

	Mitsero seamount	Akaki canyon CY1/1A	Politico	Onophrious graben
depth range studied	0-350 m	0-700 m	0-600 m	0-350 m
Oldest sediment*	≤23 Myr[#]	≤70 Myr	≤70 Myr	~90 Myr
Seafloor topography	high	normal	normal	low
Dominant lithologies	pillows and sheets	pillows and sheets	pillows and sheets	sheet flows

985 Summary of the study areas. *best estimate. [#]Excluding umbers patches.

986

Figure 1

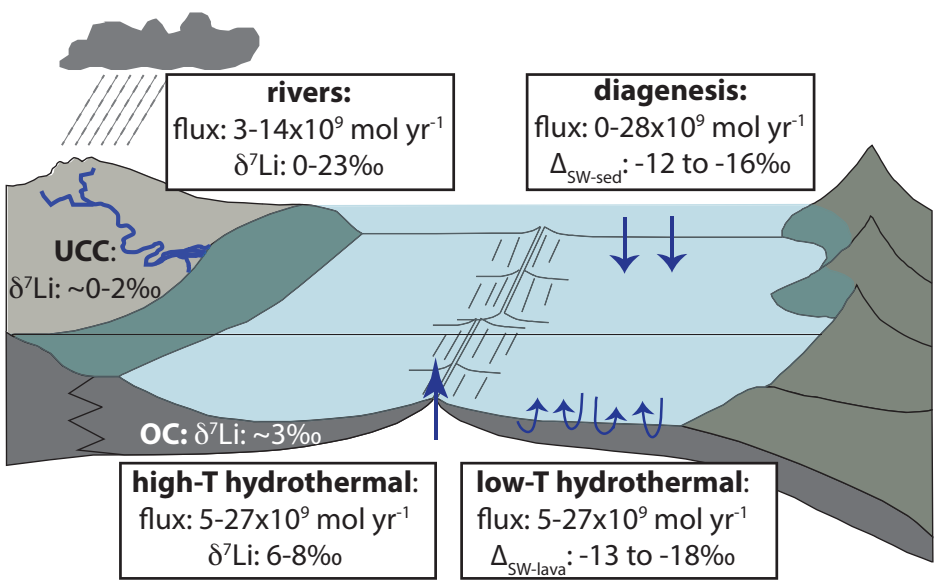
rivers:
flux: 3-14x10⁹ mol yr⁻¹
δ⁷Li: 0-23‰
diagenesis:
flux: 0-28x10⁹ mol yr⁻¹
Δ_SW-sed: -12 to -16‰
UCC:
δ⁷Li: ~0-2‰
OC: δ⁷Li: ~3‰
high-T hydrothermal:
flux: 5-27x10⁹ mol yr⁻¹
δ⁷Li: 6-8‰
low-T hydrothermal:
flux: 5-27x10⁹ mol yr⁻¹
Δ_SW-lava: -13 to -18‰

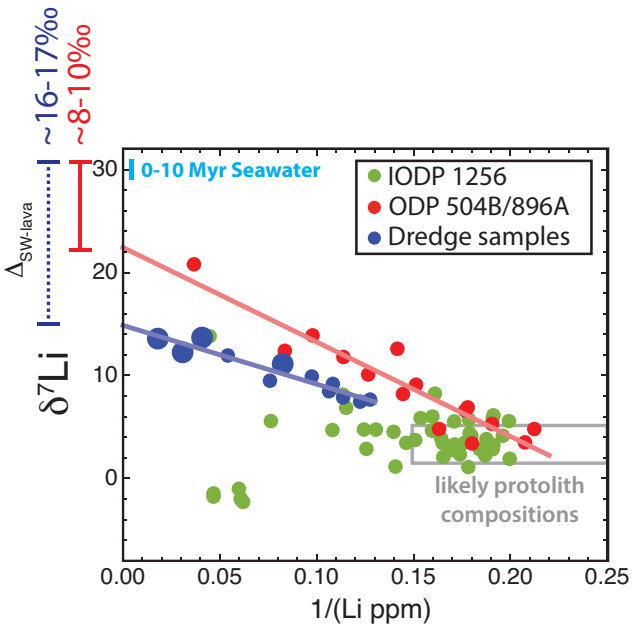
~16-17‰
~8-10‰
Δ_SW-lava
δ⁷Li
0-10 Myr Seawater
IODP 1256
ODP 504B/896A
Dredge samples
likely protolith compositions
30
20
10
0
0.00
0.05
0.10
0.15
0.20
0.25
1/(Li ppm)

Figure 2

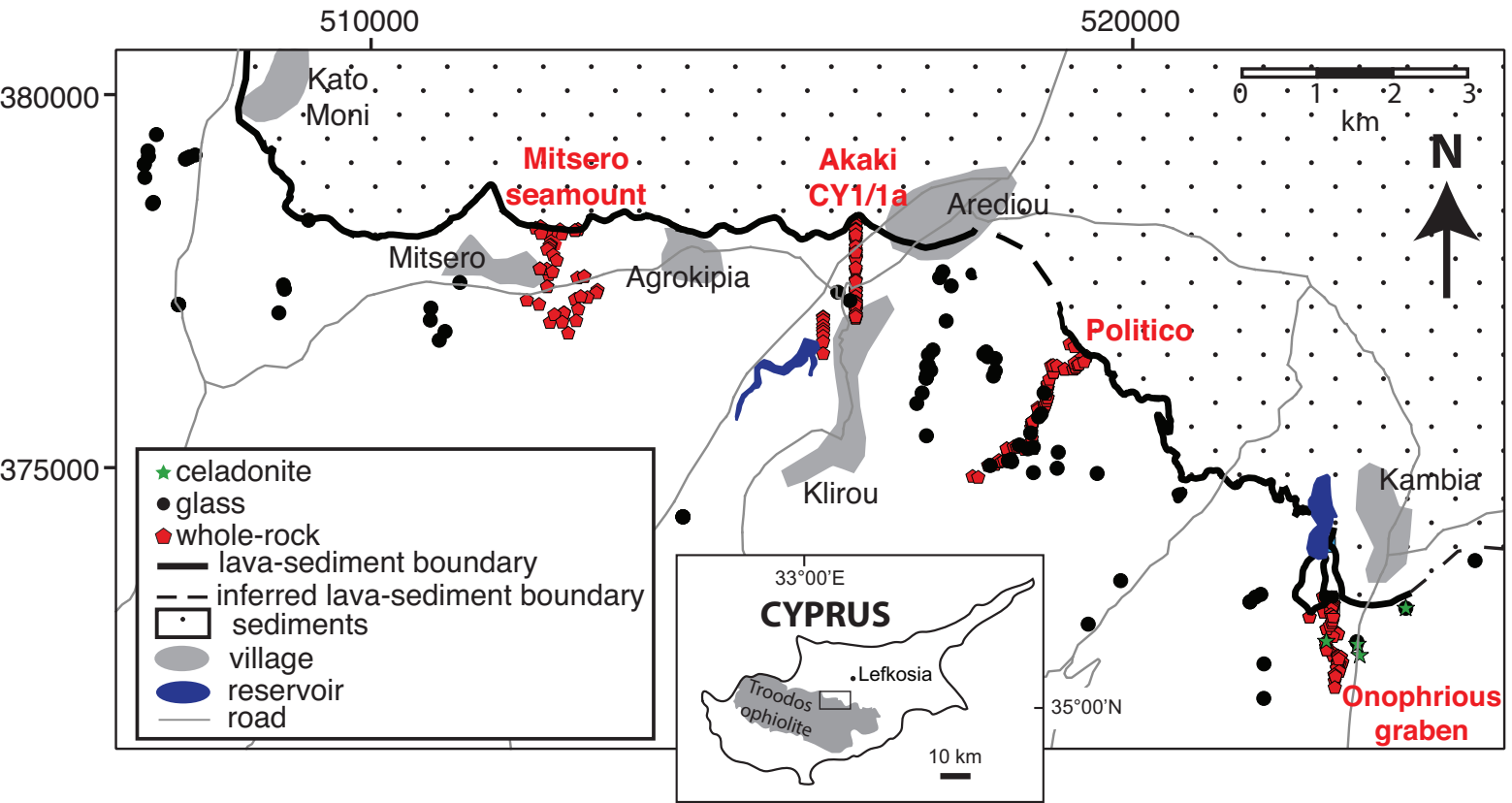
510000
520000
380000
375000
Kato
Moni
Mitsero
seamount
Akaki
CY1/1a
Arediou
Mitsero
Agrokipia
Politico
Klirou
Kambia
Onophrious
graben
0 1 2 3
km
N
celadonite
glass
whole-rock
lava-sediment boundary
inferred lava-sediment boundary
sediments
village
reservoir
road
33°00'E
CYPRUS
Lefkosia
Troodos
ophiolite
10 km
35°00'N

Figure 3

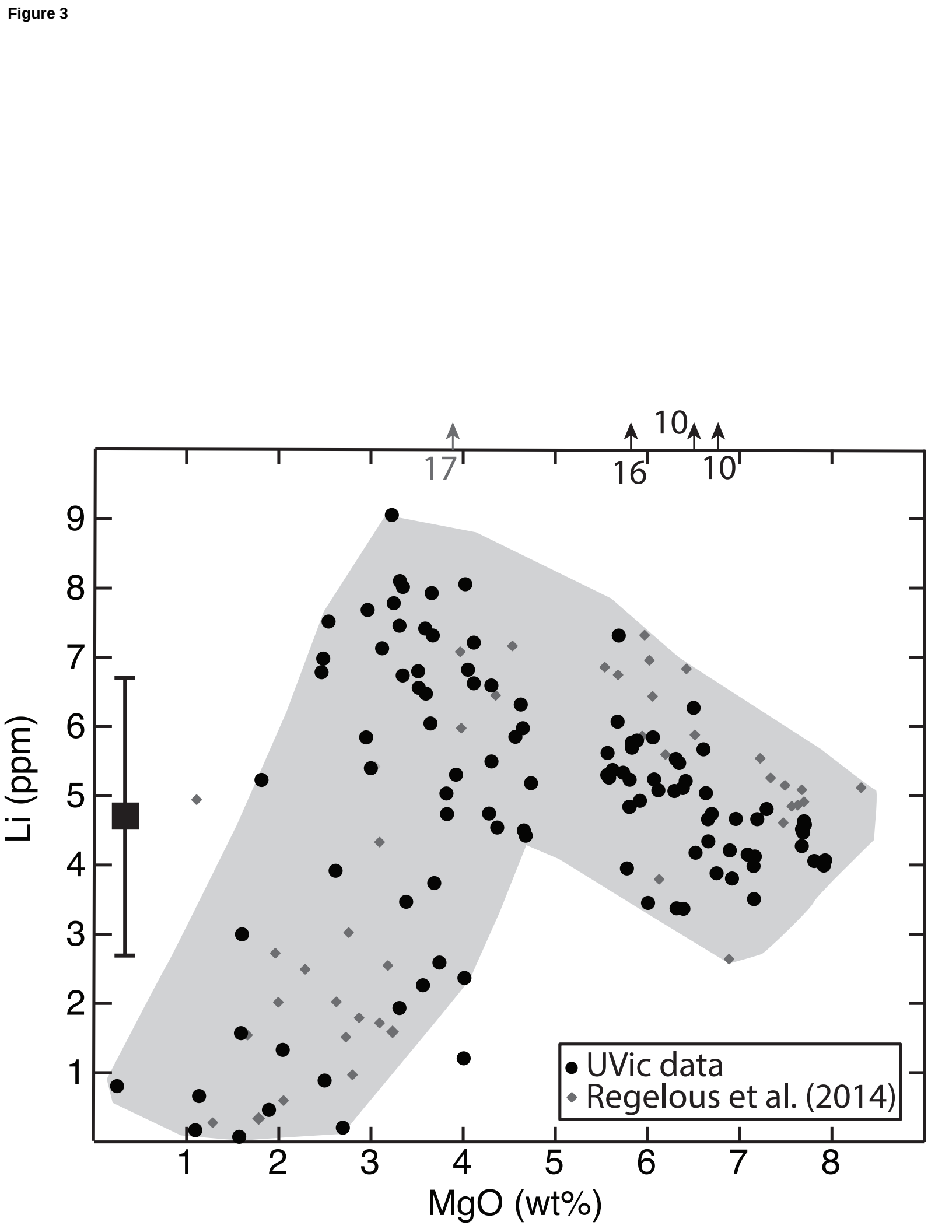
17
16
10
10
9
8
7
6
5
4
3
2
1
Li (ppm)
1
2
3
4
5
6
7
8
MgO (wt%)
UVic data
Regelous et al. (2014)

Figure 4

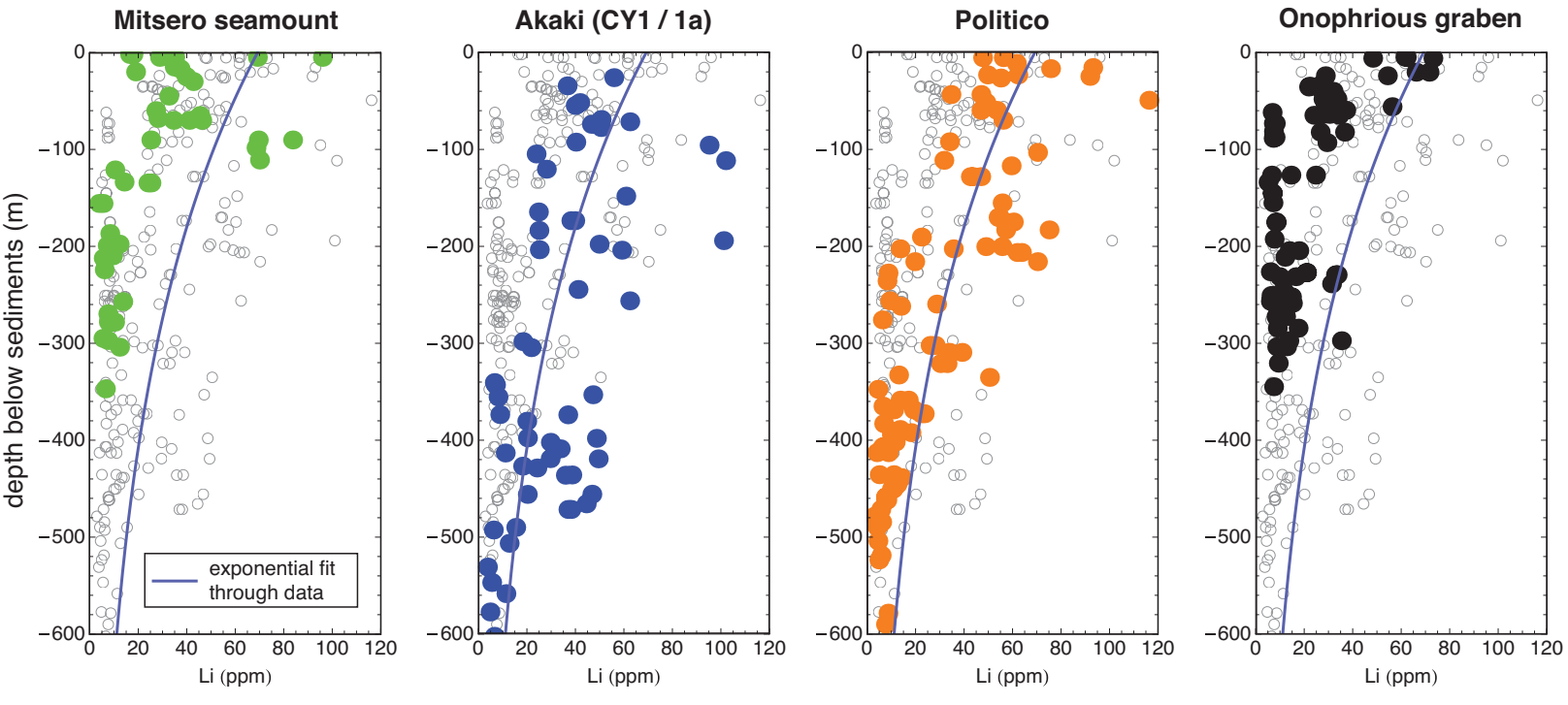
Mitsero seamount
Akaki (CY1 / 1a)
Politico
Onophrious graben
depth below sediments (m)
0
−100
−200
−300
−400
−500
−600
0
20
40
60
80
100
120
Li (ppm)
exponential fit
through data

Figure 5

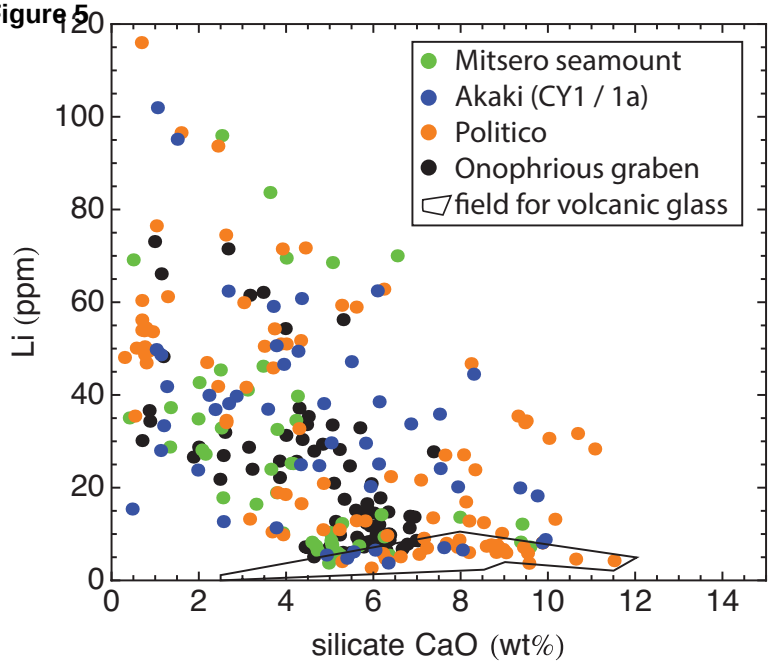
Mitsero seamount
Akaki (CY1 / 1a)
Politico
Onophrious graben
field for volcanic glass
Li (ppm)
silicate CaO (wt%)

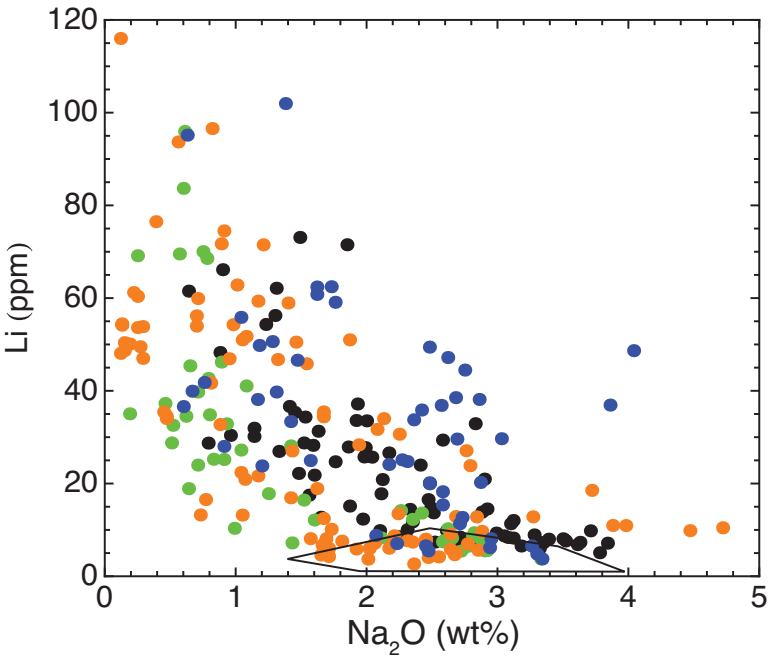
Li (ppm)
Na2O (wt%)

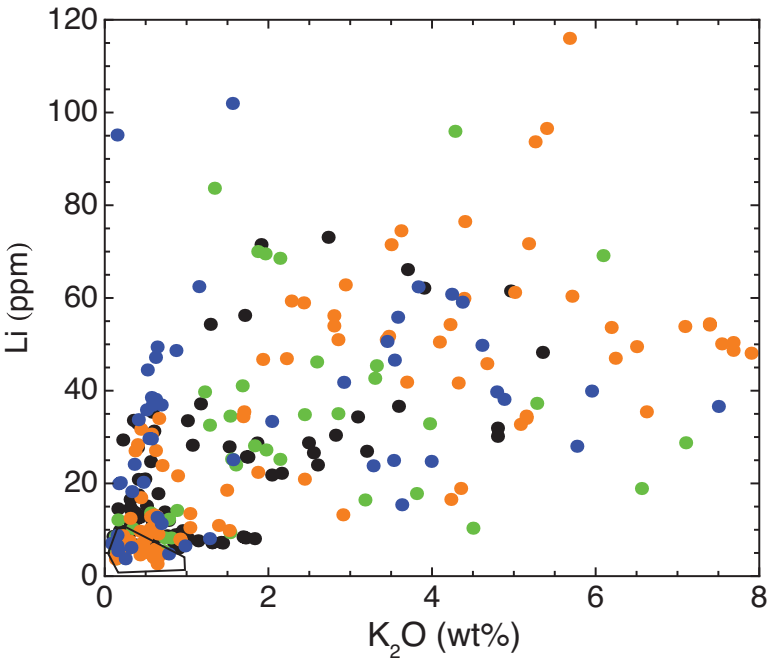
Li (ppm)
K2O (wt%)

Figure 6

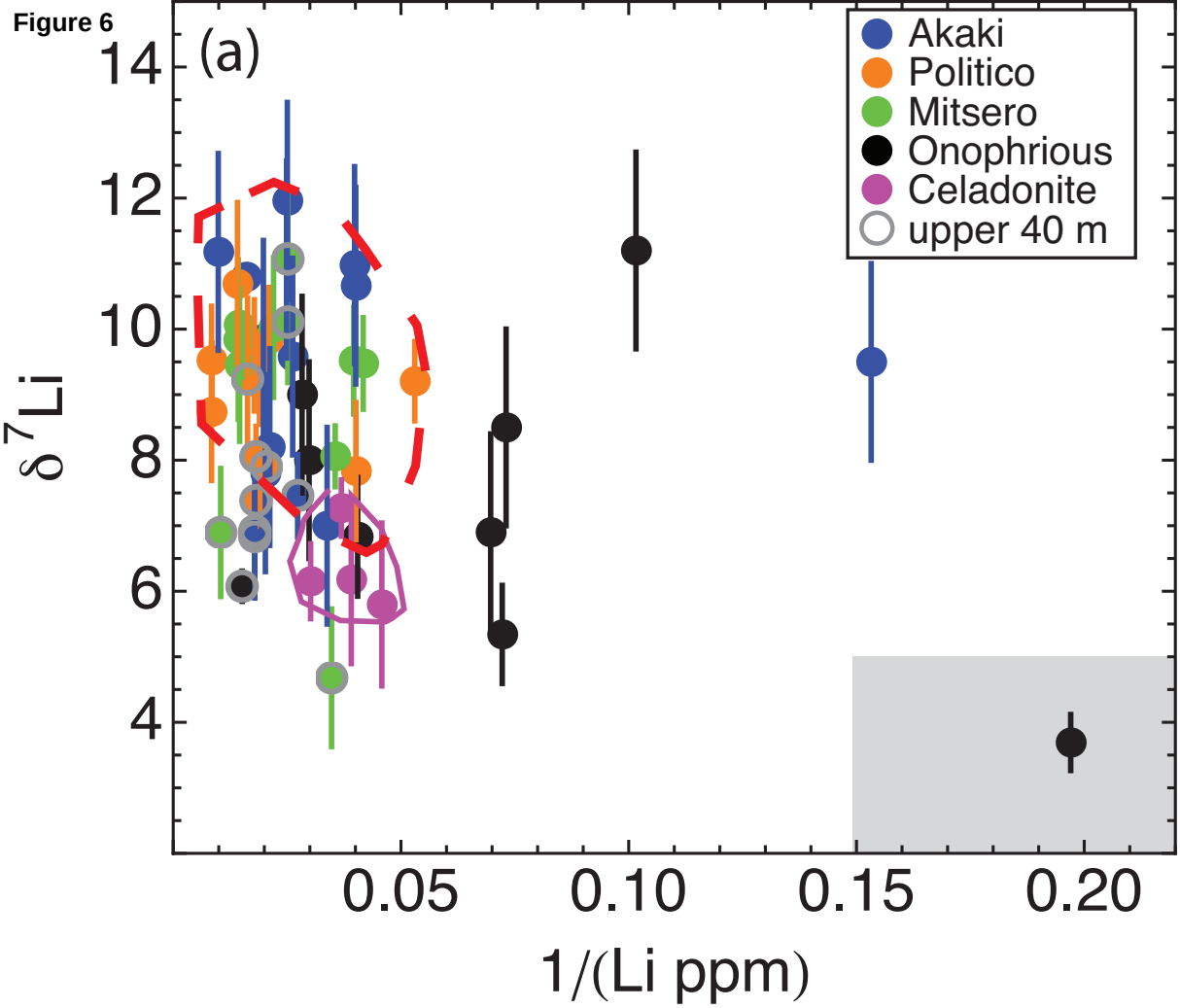
(a)
Akaki
Politico
Mitsero
Onophrious
Celadonite
upper 40 m
δ7Li
1/(Li ppm)
14
12
10
8
6
4
0.05
0.10
0.15
0.20

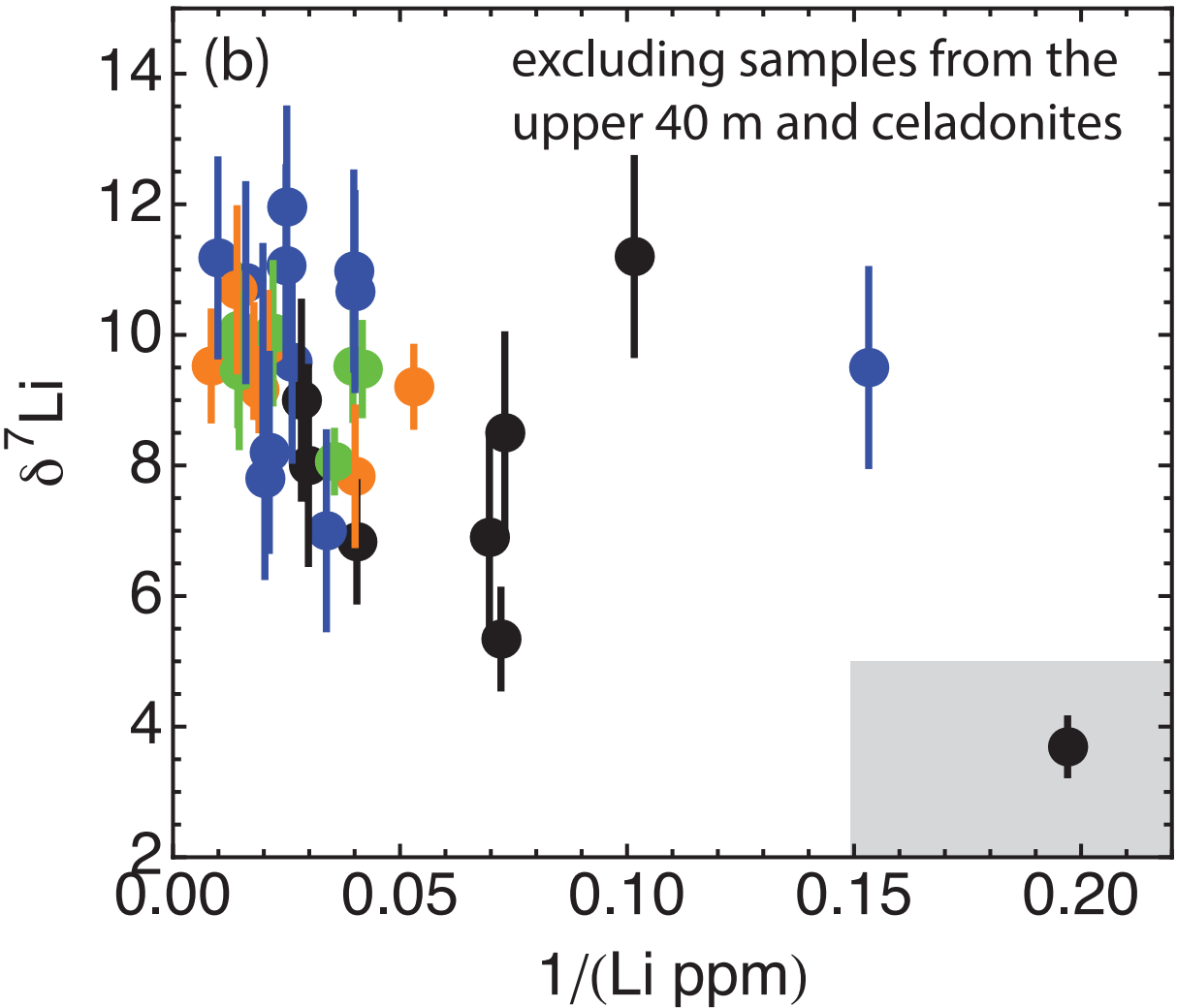
(b)
excluding samples from the
upper 40 m and celadonites
δ7Li
1/(Li ppm)
14
12
10
8
6
4
2
0.00
0.05
0.10
0.15
0.20

Figure 7

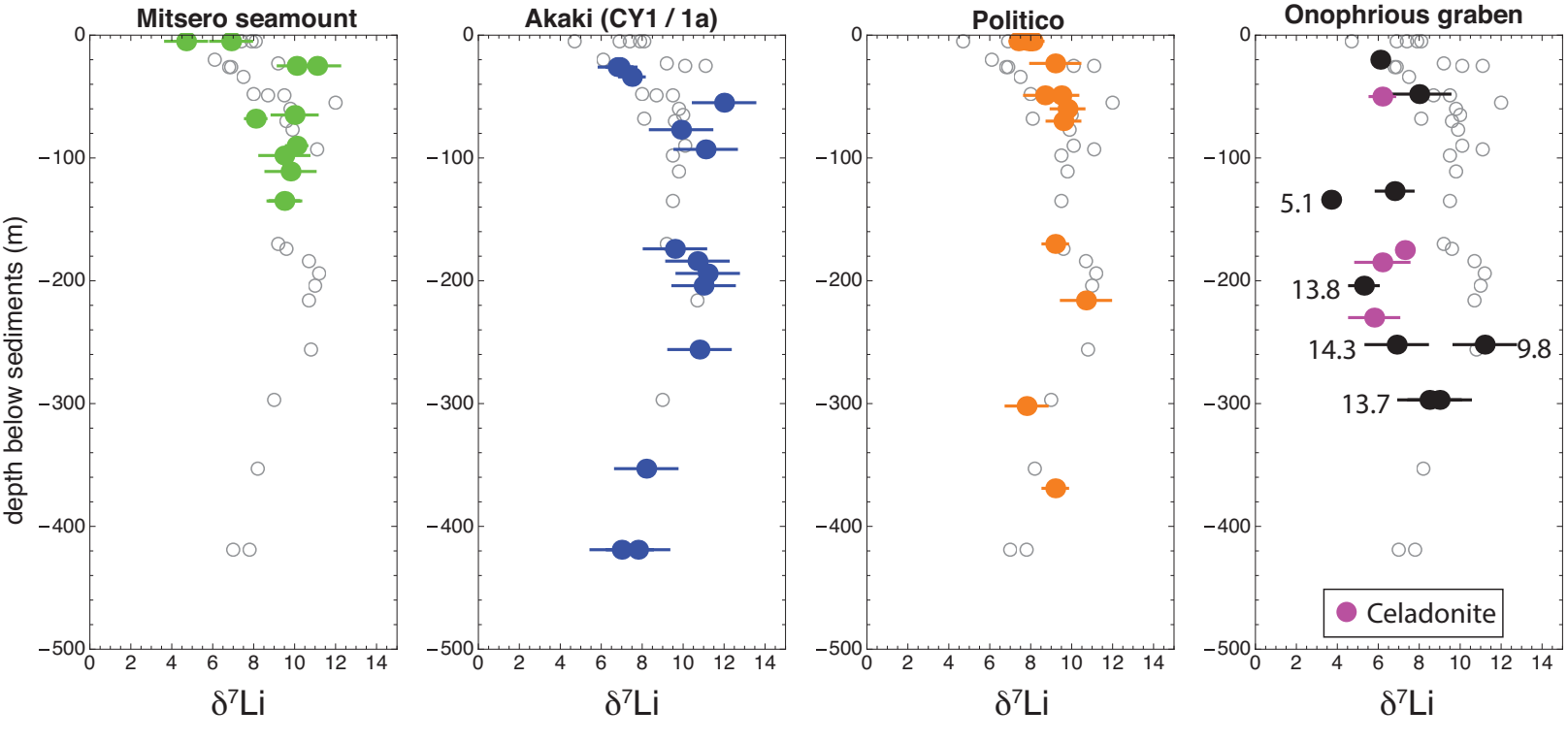
Mitsero seamount
Akaki (CY1 / 1a)
Politico
Onophrious graben
depth below sediments (m)
0
−100
−200
−300
−400
−500
0 2 4 6 8 10 12 14
δ7Li
5.1
13.8
14.3
9.8
13.7
Celadonite

Figure 8

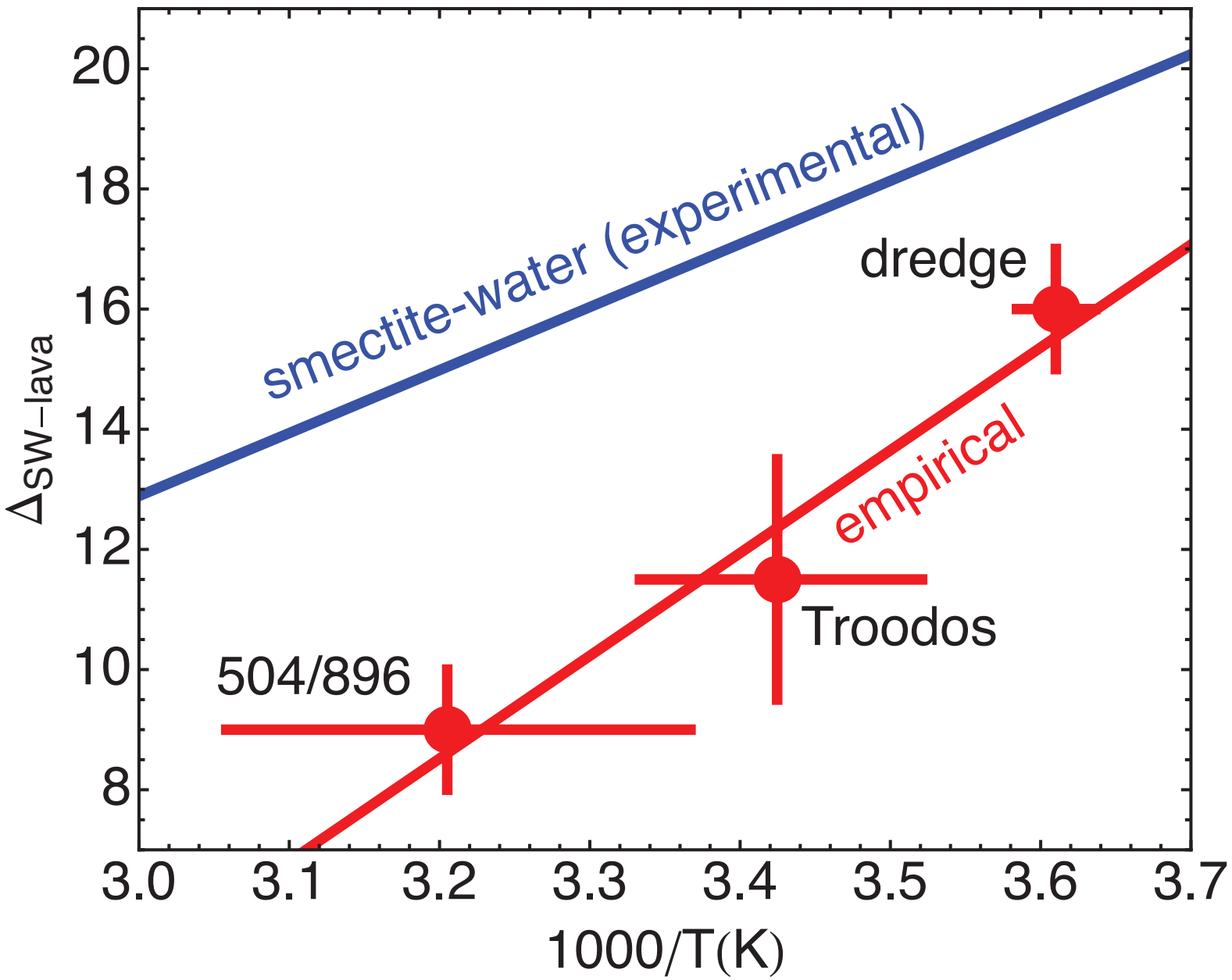
20
18
16
14
12
10
8
$\Delta_{SW-lava}$
smectite-water (experimental)
dredge
empirical
Troodos
504/896
3.0
3.1
3.2
3.3
3.4
3.5
3.6
3.7
1000/T(K)

Figure 9

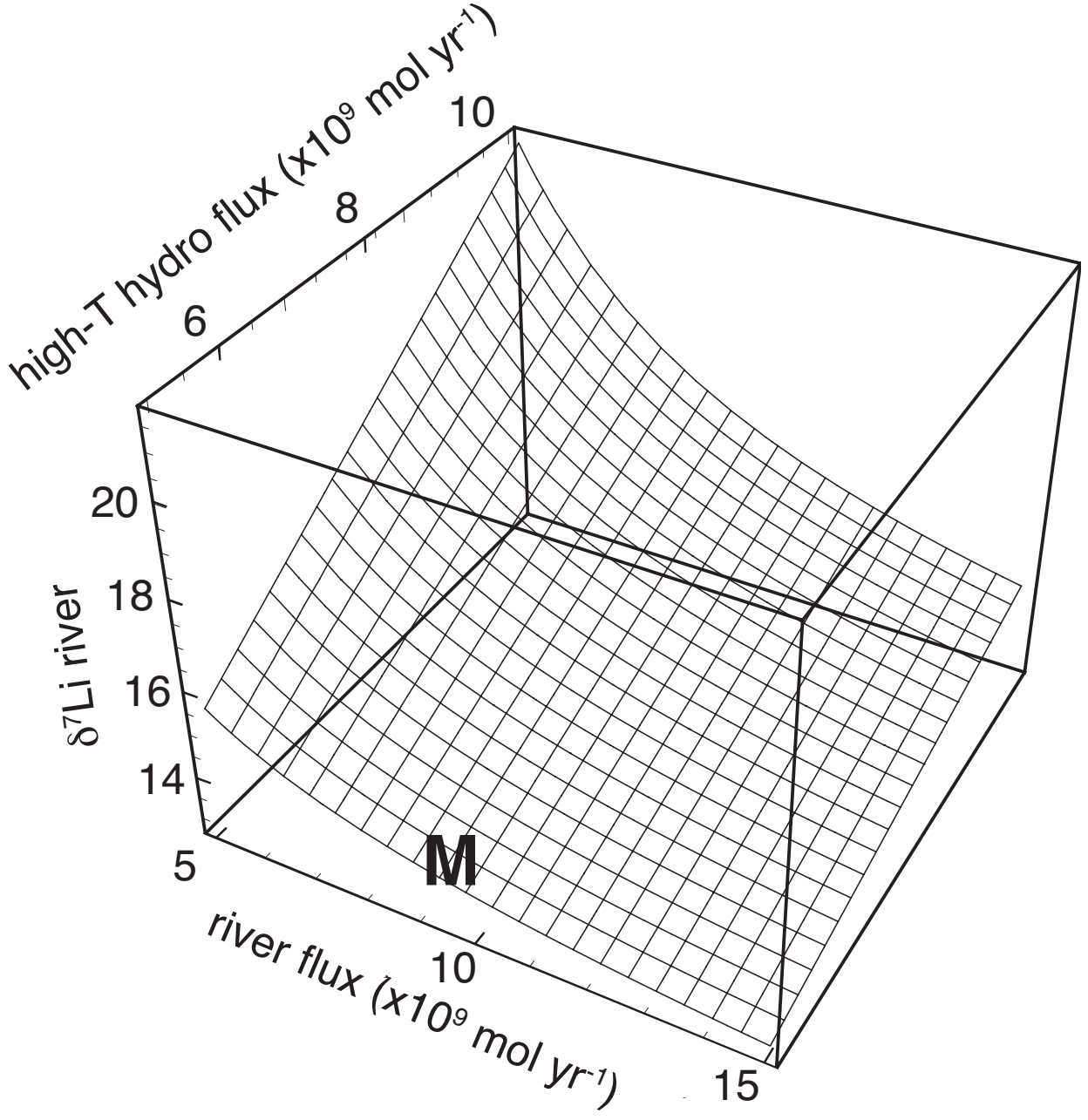
high-T hydro flux (x10⁹ mol yr⁻¹)
6
8
10
δ⁷Li river
20
18
16
14
5
river flux (x10⁹ mol yr⁻¹)
10
15
M